UNIVERSITÀ DEGLI STUDI DI UDINE

CORSO DI DOTTORATO DI RICERCA IN

SCIENZE BIOMEDICHE E BIOTECNOLOGICHE CICLO XXV

TESI DI DOTTORATO DI RICERCA

A NEW SCAFFOLD ENRICHED WITH MESENCHYMAL STEM CELLS FOR TREATMENT OF BONE DEFECTS

DOTTORANDO
DR. PAOLO DI BENEDETTO

RELATORE
CHIAR.MO PROF. FRANCESCO CURCIO

CORRELATORE
DR.SSA ORNELLA GONZATO

ANNO ACCADEMICO 2012/2013

Index

Abstract

Background
The repair of large bone defects remains a major clinical orthopedic challenge. The engineering of bone tissue and use of mesenchymal stem cells (MSCs) offer new therapeutic strategies to aid musculoskeletal healing. The delivery of viable stem cells to site of bone defect is an important area of biomedical research.
Objectives
The aim of this study was to evaluate the regeneration of bone as well as the local tolerance of a new scaffold composed by polycaprolactone-tricalcium phosphate loaded or not with mesenchymal stem cells.
Matherials and methods
In the first experiment we evaluated the in vivo local tolerance and the ectopic bone formation in mice (nod/scid) implanting the scaffold loaded or non-loaded with stem cells and using hydroxyapatite scaffold as control. Histological evaluation was performed at 8 and 12 weeks from the implantation. In the second experiment we focused on the osteointegration capability of this scaffold enriched or non-enriched autologous stem cells (expanded in bioreactor) in rabbit. The protocol consists of 5 experimental groups of animals (adult New Zealand white rabbit), all with a single implant site per animal. Each leg will be x-rayed in the immediate postoperative time and then every 4 weeks for a total of 4 radiographs for each animal. Histological evaluation was performed at 8 and 12 weeks from the implantation. In the last experiment we evaluated osteointegration and local tolerance of this scaffold enriched or not of autologous stem cells (expanded in vitro in bioreactor) in sheep. The protocol consist of 2 groups of 7 experimental animals each one. Conventional x-ray, micro-CT and histological evaluations were done.
Result
The scaffold composite by PCL/TCP investigated in this study showed a good behavior in vivo. In fact, none of the samples analyzed in this study induced even a minimal inflammatory reaction in mice, rabbit, and sheep models. Moreover PCL/TCP scaffold showed good vascularization and osteointergration in all specimens when implanted in bone defect.
Conclusions
In the present study the bioabsorbable PCL/TCP scaffold enriched of MSC shows to promote new bone formation and to be well tolerated by host (no inflammatory reaction was seen).
More studies are needed to confirm these results.

Introduction

With the increasingly active lifestyle, accidents and aging population, oral and maxillo-facial treatment, orthopedic solutions encompassing joint and bone repair, fractures and bone tumors remain to be in the greatest demand. Bone is the second most transplanted tissue in the world.

The immense need for bone grafts and substitutes have been forecasted to reach $3.3 billion of revenues by 2013, with a compound annual growth rate of 13,8% from 2006 to 2013 in the USA. [1]

Despite the innate capacity of bone tissue for regeneration upon damage, mechanical or metabolic restrictions often necessitate augmentation of natural fracture repair. Such restrictions can include non-unions, delayed-unions, and bone loss due to trauma or tumor resection. [2] Repair and regeneration of critical size bone defects are challenging, and are hampered by frequent suboptimal outcomes.

In facilitating bone repair in large defects, viable autologous bone graft remains the gold standard. Its use, however, is severely limited by donor site morbidity and, in diseased patients, inadequate volume or quality of graft materials. To date the alternative in orthopedic reconstructive surgery has been the use of allograft bone. However, allogenic bone tissue has not the osteoinductive capacities of autograft and this, together with the incomplete remodeling and the potential risk of pathogen transmission has restricted its indications for orthopedic applications.

Regenerative medicine has emerged as a promising approach for the restoration of function in damaged or diseased skeletal tissue. Bone scaffold, compared with autogenous bone grafts, is less invasive, has not need of donor site and has potential for creating customized grafts.

In the last decade interest on it has grown developing a wide variety of biomaterials with different physico-mechanical, chemical and biochemical properties. Despite significant advances in this field, the development of biomimetic scaffolds for bone tissue generation and osteointegration has remained a challenge for researchers. Depending on the application, bioresorbable and non-bioresorbable polymers are used. In applications that require only temporary presence of the scaffold, such as bone tissue grafts, is indicated the use of bioresorbable polymers. Among bioresorbable polymers are homopolymers and co-polymers based on poly lactic acid, poly glycolic acid and poly caprolactone. Up to date, poly-caprolactone is regarded as a soft and hard tissue compatible bioresorbable material and it has been considered as scaffold for fibroblast and osteoblast growth.

Bone physiology, fractures healing and bone defects.

A simple general rule serves as a key for understanding the structural varieties in bone development, growth and fracture healing: bone is deposited only on a solid core. In fact, the elaboration of highly organized bone matrix, and especially its mineralization, requires mechanical rest.

This rest is biologically provided by the formation of a scaffold. In addition, bone formation is dependent on an adequate blood supply, and osteoblasts function properly only near by capillaries.

Bone retains an inherent capacity for controlled growth, remodeling in response to mechanical stimulations and regeneration upon damage providing. [3]

It is often noted that bone repair process is, to a large degree, a recapitulation of skeletal developmental events. [4] Repair involves both intramembranous ossification, which occurs under the periosteum a few days after fracture, and endochondral ossification occurring adjacent to fracture site over a period of up to 4 weeks. Remodeling of the woven bone over several weeks follows this. New bone tissue is morphologically and physically indistinguishable from the intact bone surrounding itself. [2, 5]

If vascularization is temporarily interrupted or put at risk by mechanical forces and motion, osteoblasts are inclined to change their genes expression and become fibroblasts or chondroblasts. The healing pattern of bone defects provides an excellent model for the study of the natural course of bone regeneration in mechanically wholesome sites and under good blood supply. This way of healing is, for obvious reasons, of clinical interest. Open reduction and internal fixation aim to achieve a close adaptation and stable fixation of the fragment ends. It results in direct (or primary) fracture healing without any alternative way with cartilage formation and endochondral ossification. The pattern of defect repair also

characterizes the incorporation of bone grafts as well as the osteointegration of orthopedic and dental implants, where primary stability and precise fitting are essential to succeed.

Healing of small cortical defects was investigated microscopically in bore holes of 0.1 to 1 mm diameter in the cortex of tibial bones in rabbits. [6]

Defect healing, in these holes, starts with bone formation within a couple of days without preceding osteoclastic resorption. Woven bone is deposited, upon the wall of the holes. Holes with a diameter of 200 μm or less are then concentrically filled, like secondary osteons. Instead, a scaffold of woven bone bridges larger holes within the first 2 weeks. Then parallel-fibered bone and lamellar bone are deposited upon the newly formed trabeculae until the inter-trabecular space is almost completely filled. It needs about 4 to 6 weeks to complete the final healing process. The outset value for this rapid bridging is around 1 mm in rabbit cortical bone. [7] Larger holes cannot be covered instantly or, in other words, by one single jump (" osteogenic jumping distance''). [8] This does not mean that the holes stay permanently open, but it takes longer time to complete the filling process. The compact bone that fills the holes at 4 to 6 weeks is considerably different from the original cortex. Complete healing in the sense of full restoration of the original structure can be achieved only by haversian remodeling, which starts in the second and third months and continues for months if not years.

The outline of the repair of small cortical defects can be divided into three steps that closely resemble the stages of formation of compact bone during skeletal development and growth. Initially, the defect is bridged with woven bone. The resulting structure is then reinforced by parallel-fibered and lamellar bone, and finally haversian remodeling restores the original structure. However, healing capacity of bone defects has its limitations.

Bore hole experiments have shown that exists a critical value for the defect size. If this value is surpassed, the defect persists, at least partially. The actual dimension of critical size defects varies considerably, depending on species, age and anatomical site. Therefore, the critical size

of defects has to be specifically defined in animal studies. Another important aspect is the containment of the defect: bony walls and open communications with the bone marrow space are more advantageous for a bony filling than contact with connective tissue elements. Conditions that block or prevent bone repair include (1) failure of vascular supply, (2) mechanical instability, (3) oversized defects, and (4) competing tissues of high proliferative potential. Different procedures are established for promotion of bone repair in oversized defects and for the prevention of fibrous tissue ingrowth. [9]

Regenerative medicine: current strategies

Regenerative medicine is a relatively new, highly promising field of reconstructive biology that approaches the recent advances in medicine and surgery, polymeric chemistry and physiology. In this field, regenerative medicine may include the use of synthetic polymers to facilitate the initial healing processes. In fact, there has been increased interest in scaffold-based strategies as represented by the exponential rise in number of publications over the last years.

The fundamental concept underlying regenerative medicine is to combine a medical device like a scaffold with living cells or growth factors to form a construct, which promotes the repair or regeneration of tissues. The scaffold is used for his osteoconductive properties [10] [11] and the cells or growth factors are used for their osteoinductive or osteogenic properties. [12] [13]

Various scaffolds, used in combination with stem cells or gene therapy strategies, have shown promising results in terms of new bone tissue formation and repair of segmental defects in animal studies. [14] Other in vitro and in vivo studies have shown excellent biocompatibility and bone regeneration for several different types of bone scaffolds. However some critical issues still remain: biocompatibility and biomechanical properties in polymeric scaffolds, limited bioactivity, biodegradation, and metal ion release for metallic scaffolds, toughness as well as reliable and production techniques for ceramic scaffolds. [15]

In addition, the control of degradation rate of any scaffold materials requires better understanding to match the regeneration rate of the replacing bone tissue.

Scaffolds are designed with interconnected porosity in which osteogenic and angiogenic agents are added. However, organization of porosity in the scaffold can play a significant role in the quality of bone formation. [16]

Scaffolds

Right design and material properties require further investigations to design more clinically useful scaffolds. The requirements of the scaffolds also need to be suited accordingly to the different types of bone defects and fracture sites.

The polymer choice, characterization, technique of realization of the structure and interaction structure/cells is very important topics in this field.

The general criteria in designing an appropriate scaffold for bone tissue include choice of material, architecture and porosity, surface chemistry and osteoconductivity as well as mechanical strength. Reproducibility of manufacturing process and clinical handling are also essential. First of all, the material needs to be biocompatible, biodegradable and must have physical and mechanical properties similar to bone tissue. Moreover, it must not give adverse physiological response from the host. Ideally, the scaffold should serve as a temporary structure, which subsequently degrades in combination with new bone tissue formation over time.

Types of scaffold

There has been a clear increase in the number of new scaffolds that have been developed for bone tissue over the last years, using different materials and designs.

Polymers are the most commonly studied materials, followed by ceramics and often used in combination as composites.

Factors that have to be considered for the choice of the polymer are:

1) to be biodegradable, or to be removable through the normal metabolic processes;

2) to be biocompatible;

3) to be recognized by cellular receptors;

4) interaction with other molecules of the extracellular matrix;

5) its degradation products must be removed by cells (macrophages);

6) a degradation time sufficiently long, but not excessive;

7) absence of toxicity;

8) suitable mechanical properties and mechanical stability for an appropriate time;

9) reproducible and standard manufacturing process;

10) to be easily sterilized in order to avoid contaminations and infections;

11) chemical and physical properties to ensure cellular functions (adhesion, growth).

Biocompatibility of a scaffold is described as its ability to support normal cellular activity, including molecular signaling systems, without any local and systematic toxic effects to the host tissue. [17] A bone scaffold must be also osteoconductive. The scaffold has to allow the bone cells to adhere, proliferate, and form extracellular matrix on its internal and external surface. The scaffold should also have osteoinductive properties that mean to be able to induce new bone formation through biomolecular signaling and recruiting progenitor cells. Furthermore, an ideal scaffold has to form blood vessels in or around the implant within few weeks after implantation to actively support nutrient, oxygen, and waste take off.

The mechanical properties of an ideal bone scaffold should match host bone properties. A proper load transfer is important as well. Mechanical properties of bone vary widely from cancellous to cortical bone. Young's modulus of cortical bone is between 15 and 20 gpa and that of cancellous bone is between 0.1 and 2 gpa. Compressive strength varies between 100 and 200 mpa for cortical bone, and between 2 and 20 mpa for cancellous bone.

The large variation in mechanical property and geometry makes it difficult to design an ideal bone scaffold.

Essential property for scaffolds is interconnected porosity, where the pore size should be at least 100 μm in diameter for successful diffusion of nutrients and oxygen for the survival of the cells. [18]

However, pore sizes in the range of 200–350 μm are found to be optimum for bone tissue ingrowth. [19]

Furthermore, more recent studies show that multi-scale porous scaffolds, involving micro and macro porosities, can give better results than only macro porous scaffolds. [20] Unfortunately, mechanical properties such as compressive strength are reduced by porosity. Moreover porosity increases the complexity for easy and reproducible scaffold manufacturing. Researchers have investigated porous scaffolds using polymers, ceramics, composites, and metals. Nonetheless bio-ceramic materials strength matches close to the cortical bone and some polymers to that of cancellous bone, ceramic–polymer composite scaffolds are usually weaker than bone. Porous metallic scaffolds meet the mechanical requirements of bone, but fail in providing the necessary implant-tissue integration and add the issues related to metal ion leaching. [21]

In bone tissue regeneration another important concern for scaffolds is bioresorbability. [22] An ideal scaffold should not only have mechanical properties closed to that of the host tissue, but also should have a controlled resorption rate, similar to bone tissue regeneration rate. The degradation behavior of the scaffolds should be variable based on applications. In spinal fusion it could be 9 months, in cranio-maxillofacial surgery 3–6 months for example.

In the end, the keys challenge in designing and manufacturing a multi-scale porous scaffolds are the ideal composition, targeted biomolecules, mechanical properties and related bioresorbability. [23]

Polymers

Biodegradable polymers represent the category of materials that are mostly used in bone regenerative medicine for manufacturing of scaffolds. They are available in a range of compositions, properties, and forms (solid, fibers, fabrics, films and gels) and can be easily molded into different shapes and complex structures. The molecule of a polymer is constituted by the union of a large number of simple units called monomers through polymerization reaction. Their ability to support tissue growth and remodeling over their function should be the principal reason of using biodegradable polymers [24]

Polymers can be classified according to the following criteria:

- mechanisms of polymerization, which are divided into polyaddition and polycondensation;
- molecular weight, which is defined as the molecular weight of the monomer multiplied by the degree of polymerization;
- structure of the chains (linear, branched and cross-linked);
- crystallinity;
- thermodynamic properties;
- structures of co-polymers.

Natural polymers such as chitosan, hyaluronic acid, collagen have a low immunogenic potential, with a bioactive potential that has the capability to interact with the host surrounding tissue. [25]

Synthetic polymers have important advantages due to their suitable biodegradation rate, higher predictability of properties, better lot-to-lot consistency. They could also be easily fabricated and shaped as needed. [24]

Both natural and synthetic polymers are bioactive and biodegradable [23], consequently they are ideal for use as scaffolds in tissue engineering.

Natural polymers, commonly used for bone tissue regenerative surgery, are hyaluronic acid, collagen, silk, fibrin, chitosan and alginate. [26] Despite some disadvantages, these polymers are frequently used in scaffolds production. Collagen, for example, which is a fibrous protein, could present several disadvantages such as: potential pathogenic transmission, poor mechanical properties, antigenicity, and poor handle ability. Synthetic polymers used for tissue engineering applications include polyethylene glycol (PEG), poly-glycolic acid (PGA), poly-lactic acid (PLA), poly-caprolactone (PCL) and copolymers of lactic acid-glycolic acid (PLGA) and (PLLA-PDLA). Degradation of these polymers produces monomers, which are removed by the physiological pathway. [15]

Polymers degrade primary by chemical reactions like hydrolysis and only minimally by enzymatic and cellular pathways. Therefore, co-polymerization and changes in hydrophobicity and crystalline structure can change degradation predictability. The fast diffusion of water into the material can cause a degradation reaction that is not only limited to the surface but takes place in the whole volume (bulk-degradation). Instead, hydrophobic polymers only degrade from the surface (surface-degradation). [27] Some of the products caused by degradation, like micro crystallites, may also cause immunological and foreign body reactions.

Erosion particles of biological inert polymers can activate macrophagic response causing osteolysis without additional chemical reactions. An in vivo study on rabbits shows that after implantation of polymer screws the drill holes were not refilled with trabecular bone after 54 months, despite their complete degradation. [28]

Even with high initial strength, polymeric scaffolds show accelerated strength degradation in vivo. [29]

Poly-glycolic acid (PGA) and poly-lactic acid (PLA) have different characteristics. PGA is broadly used for scaffold production. As a result of its hydrophilic nature, poly-glycolic acid

degrades rapidly in vivo or in aqueous solutions and it loses its mechanical properties in about 2 to 4 weeks. On the contrary, poly-lactic acid has a chemical structure (semi crystalline), which enables it to have more hydrophobic properties and allows for resistance to hydrolysis. Both in vivo and in vitro conditions, poly-lactic acid takes months or years to lose mechanical integrity.

All linear aliphatic polyesters derived by lactic acid and glycolic acid are poly α-hydroxyl acids. There are also linear aliphatic polyesters based on poly ω-hydroxy acids. These are polycaprolactone (PCL), poly β-hydroxybutyrate (PHB), poly-β-hydroxyvalerate (PHV) and copolymers PHB/PHV. The polycaprolactone is another polymer widely used. Speed of degradation of polycaprolactone is slow; therefore, polycaprolactone is suitable for long-term implants.

Polymers have limited capabilities in achieving strong bonding and integration with bone. Moreover, they exhibit elastic moduli between 7mpa (for elastic materials) and 4gpa (for stiff polymers), which is lower than cortical (17gpa) and cancellous bone (0,1-2 gpa) elastic moduli. [30]Furthermore, because of their low elastic moduli, polymers are predisposed to a deformation mechanism called creep, which can be significant even at stresses below their individual yield strength and at room temperature. [23] [30] In addition, degradation of some polymers such as poly-glicolic acid (PGA) and poly-lactic acid (PLA) results in a local acidic environment that can have adverse host tissue response. [15]

Metals

Metals and alloys widely used as biomaterials include gold, titanium, stainless steel, and titanium alloys. Porous metallic scaffolds have been examined as bone graft materials. [31] [32] metals have outstanding fatigue resistance and high compressive strengths. Nevertheless, these scaffolds are not biodegradable and biomolecules cannot be integrated into them. Furthermore, there are issues related to metal ion release.

Metals like titanium and stainless steel are biocompatible, they exhibit high strength, and they are easy to shape and relatively inexpensive. The main disadvantages of stainless steel and titanium are that they are not bioresorbable and they are rigid. The higher Young's modulus of these metals induces stress shielding which could inhibit the native tissue from mechanical stimulation. Mechanical stimulation is an important initiator of osteoblastic differentiation and activation. For these reasons metallic materials are solely used for scaffolds in limited situations, such as in spine surgery. A new biodegradable scaffold material has been developed recently based on magnesium alloy. It stimulates bone formation and has a suitable degradation rate as founded in a rabbit model. [33] The osteoinductive properties are primarily based on the corrosion product magnesium hydroxide, which can temporarily increase osteoblast activity and decrease the number of osteoclasts. [34]

Ceramics

The hydroxyapatite, bioactive glass, carbon, zinc oxide and titanium are examples of biocompatible ceramics. Calcium phosphate ceramics were introduced 40 years ago as bone substitutes. Actually, calcium phosphate (CaP) ceramics are widely used for scaffold production. Calcium phosphate ceramics are available in a variety of products due to different forms and chemical composition (Ca/P-ratio).

Different types of ceramics have been examined including hydroxyapatite (HA), tricalcium phosphate (TCP) and composites like biphasic calcium phosphates (BCP). Their physical properties including stability, degradation rate and processability can be changed in a particular range by using different compositions. The calcium phosphate bioactive ceramic scaffolds group is the most commonly used and has been widely investigated.

Natural bone consists of an organic and an inorganic fraction. The inorganic fraction amounts to 2/3 of the dry matter and principally includes calcium phosphate (85–90%), calcium carbonate (8–10%), magnesium phosphate (1.5%) and calcium fluoride (0.3%). Several minerals are present as apatite crystals, mainly hydroxyapatite. Among different caps, the majority of studies have been focused on hydroxyapatite (HA), β-tricalcium phosphate (β-TCP) or a mixture of ha and β-TCP, also known as biphasic calcium phosphate (BCP). [15] [35]

Calcium phosphate ceramics have an excellent biocompatibility and are bioactive, since they bind to bone and increase tissue formation. These ceramics do not offer osteogenic or osteoinductive properties. The structure and the Ca/P-ratio of the different ceramics (HAP 1,67, TCP 1,5) are similar to the mineral phase of natural bone. Consequently, ceramics induce an interface mechanism, which leads to calcium and phosphate ions release. This results in an indefinable bonding between the ceramic material and the bone, called bonding osteogenesis. Woven bone forms directly on the ceramic surface without a dividing layer of connective

tissue and is transformed to lamellar bone. Ceramics have low fracture toughness with a comparatively high Young's modulus between 7 and 234 gpa. [36]

Moreover, ceramics are prone to undergo creep like polymers and metals, but are less probable to creep in physiological conditions.

Pore size is one of the most important characteristics of ceramic scaffolds. Porosity should be similar to cancellous bone. Particular manufacturing techniques are needed to ensure the presence of interconnecting pores in ceramic materials. Depletion of ceramics depends on two different mechanisms: degradation and resorption. Degradation is a chemical process in a moist environment. Resorption is an active cellular process by osteoclasts with successive neoformation of bone. The resorption rate differs between the different types of calcium phosphate ceramics and can be affected by diverse composites and production techniques. Porous tcp-ceramics is reported to be removed with the same velocity of osseous ingrowth, while hap-ceramics are more permanent. [37] [38] Therefore hap-ceramics are mostly used as composites with other ceramics. The main disadvantage of ceramic scaffolds for their clinical use is their brittleness and low mechanical strength. If they are produced in an acceptable porous design they are lacking as a weight-bearing component. [23]

Bioglasses

Bioglasses are based on acidic oxides like phosphorus pentoxide, silicon dioxide and aluminum oxide and basic oxides such as calcium oxide, magnesium oxide and zinc oxide. A 3d network with connected pores was built after a melting process. [39] [40] They have a significantly higher mechanical strength if compared to most calcium phosphate ceramics.

Composite

Composite scaffolds are defined as those scaffolds that are made of at least 2 different materials such as polymer and ceramic. So composite scaffolds combine properties of different materials to achieve a synergic effect in their resultant properties. For example,

development of an interconnected cap-polymer scaffold has the advantages of both caps and polymers to meet physiological and mechanical characteristics of host tissue. Polymer in CaP scaffold increases toughness and compressive strength that become comparable to bone.

Architecture and porosity

Bone is a composite of collagen and hydroxycarbonate-apatite with 10-30% porous hard external layer (cortical bone) and 30-90% porous internal layer (cancellous bone). Mechanical properties of bone differ widely from cancellous to cortical bone. Bone tissue complex geometry makes difficult to design an ideal bone tissue scaffold. [15] This kind of scaffolds possesses a different function from traditional bone substitutes which integration with existing bone and equivalent mechanical strength are main design criteria. The aim of regenerative bone tissue scaffolds is to completely replace the implanted scaffold with new-formed bone tissue.

Mechanical strength of the scaffold must be appropriate to maintain the 3D structure and space upon which and within which new bone tissue is formed. For this reason, scaffold degradation, which is essential, must be controlled. Interconnected porosity in designing a scaffold play a significant role in the quality of new bone tissue formation. [15]

Scaffold porosity and pore size are related to the surface area available for implanted cells growth and for host tissue potential growth, including vascular invasion.[41, 42]

Recently, the importance of sufficient scaffold porosity has been emphasized in thick grafts to allow tissue ingrowth, vascular infiltration, and efficient mass transport for preserving cell survival. [43]

Utilizing hard scaffold materials such as calcium phosphate or titanium with defined porous characteristics several in vivo studies have been conducted to assess importance of porosity. The majority of these studies indicate pore structure is important in facilitating bone growth.

It was described that the large pore size or porosity of the scaffold allows effective nutrient supply, gas diffusion and metabolic waste removal but lead to low cell attachment and intercellular signaling. On the other hand, the small pore size or porosity could provide opposite properties of those described above. [44] [45] [46]

The optimal porosity and pore size vary depending on the application, thus considerations on a cut-off range that allow for the desired properties in scaffold-based regenerative medicine are needed.

Many studies have reported optimum pore size ranges for different kind of cells and tissues. For example, pore size of about 5 μm is the optimum for neovascularization, pore size of about 100-400 μm for bone regeneration and 200-350 μm for osteoconduction. Clearly it depends on the porosity as well as scaffold materials used. [47] [48] [49] [50]

Large pore size also enables cellular migration. [51] In contrast with macro-porosity, micro-porosity of the walls modifies scaffold surface texture, and provides a higher surface area, which is essential for subsequent protein absorption, cellular adhesion and proliferation. [52]

Architecturally, the interconnectivity of the scaffold filaments and pores is also important in sustaining nutrient transport, promoting cellular migration, cellular bridging and ingrowth of new bone tissue. [51] [52]

The transmission of shear stresses along its filaments throughout the scaffold upon exertion of biomechanical forces are dictated by continuity of the filaments. [53] Additionally, scaffold stiffness is enhanced by altering its structural architecture changing porosity. In fact, scaffold stiffness may also be suited altering polycaprolactone filament orientation in fused deposition modeling technique. [54] It was demonstrated that PCL scaffolds fabricated via selective laser sintering resulted in varying stiffness values (52 to 67 mpa) depending on the degree of porosity[55], while other studies showed that scaffold stiffness may be altered to match craniofacial anatomy by changing scaffold architecture. [56] These authors have reported that scaffold architecture plays a critical role in determining the stiffness of the scaffold.

Angiogenesis in bone tissue scaffolds

Vascularity of the scaffolds is essential. In fact, if blood vessels are not developed and the scaffold remains ischemic, the cells will die and no integration will take place. [57]

Bone is a highly vascularized tissue, so the performance of a bone tissue scaffold is dictated by its skill to induce neovascularization. [18]

Supply of oxygen and nutrients are indispensable for the survival of growing cells and tissues, within the scaffold. [58]

Although it takes weeks to form a complex network of blood vessels, the inflammatory wound healing response, after scaffold implantation, induces spontaneous vascularization. [18] Moreover, improper vascularization leads to nutrients and oxygen insufficiency, which results in cell death or non-uniform cell differentiation. [59] Various strategies have been investigated to solve vascularization problem in bone tissue scaffold, including use of angiogenic growth factors, like VEGF, and valsculogenic cell sources in conjunction with scaffold. These strategies showed to enhance neovascularization and subsequent new bone formation [60] other authors describe the use of growth factors, such as VEGF, PDGF and FGF to enhance vascularity and angiogenesis in the grafts. [61] [62]

Fabrication techniques

Exist several technologies for the production of polymeric scaffolds, which can be divided into two groups. Conventional techniques, which allow the realization of 3D biodegradable structures, but do not allow the realization of a sufficiently interconnected pores network. Among these, the textile technologies are designed to exploit the possibility of creating porous mesh through various weaves of fibers. The structures obtained by this technique have the typical behavior of biological materials. Conventional techniques for the production of scaffolds are: extrusion with blowing agents, solvent casting and gas foaming techniques. Common practices to fabricate 3D composite scaffold are solvent casting/particle leaching, thermally induced phase separation (TIPS), microsphere sintering and scaffold coating. [21] [34].

The great drawback of traditional manufacturing methods is that these techniques do not allow the construction of scaffolds with microscopic and macroscopic structures predefined nor controllable. Currently, these objectives seem to be better pursued with the latest technologies based on automatic image processing systems (CAD) and computer aided manufacturing (CAM). The non-conventional techniques of rapid prototyping, using specific software, allows to obtain structures with interconnected pores and easily reproducible. The generative manufacturing techniques hold great potential for bone scaffolds. Especially the 3D-powderbed based printing (3D-p) and the selective laser melting (SLM) techniques are apposite to produce scaffolds of individual shape. Among various construction techniques, solid freeform fabrication based techniques are probably the most commonly investigated for manufacturing 3D interconnected porous scaffolds. [63] Solid freeform fabrication is a general method in which 3D parts are printed layer-by-layer based on a computer-aided-design (CAD) file. Many commercial solid freeform fabrication techniques are available for

different materials. A cad file is created according to the architecture and porosity of the scaffold. The 3D printing system has a deposition bed, a feed bed, a powder spreader, a print head, and a drying unit. Initially, the printer head sprays the binder on the loose powder reproducing the specific cad file, followed by lowering the deposition bed and raising the feeder bed. Successively, a metallic roller spreads the powder over the binder, which then goes to the dryer. This process is repeated, layer-by-layer, until the specific part is built. [64] Then, to achieve higher mechanical strength, ceramic parts can be densified at high temperature. [65] In this category falls the selective laser sintering (SLS), which is one of rapid prototyping techniques more effective among those currently used. A laser beam is directed on a thin layer of thermoplastic powder, previously compacted by the sliding of a roller. The powder is supported by a mobile base, which, layer after layer, is lowered to favor the deposition of new powder with the consequential creation of new layers of the object. The process is repeated until the object is not completed in its entirety. The heat emitted by the laser beam causes a localized casting of dust particles under the control of a precise scanning system, thus obtaining the sintering. This process is very efficient and effective but it is rather expensive and leads to a large waste of material.

Solid freeform fabrication methods can also be applied to metallic or polymeric materials. Lens^{tm} has been used to produce porous metallic scaffold using titanium (Ti), tantalum (Ta), and their alloys. [31] In this process, a high power laser melts metal powder particles that are injected on the substrate at the focal point of the laser. The liquid metal is used to build parts layer-by-layer. [31, 66] This process is repeated until a 3D porous scaffold is formed. [63]

Another technique is the electro-spinning of the polymeric scaffold, which showed great promise. In this technique, polymer solution is injected through a needle under an electric field where a spinning surface gives shape to the scaffold. [34] Although it was initially designed for polymeric scaffolds, ceramic–polymer composites were also successfully

fabricated using this method. [67]

The micro molding is another unconventional technique. This is a technique of casting based on thermoplastic polymers deformation. The polymer is "injected" into a mold of the shape of the scaffold to be obtained.

Stem cells

Stem cells offer the promise of an unlimited source of cells for therapeutic applications in various conditions, including metabolic, degenerative and inflammatory diseases, cancer and for the treatment of a tissue loss. Several types of stem cells can be isolated, expanded and/or differentiated in vitro, and successively administered to the patient. Stem cells can be defined as cells with the capacity for self-renewal and the ability to differentiate into various lineages. Stem cells are able to proliferate even as stem cells in an undifferentiated form. Those that are of interest for applications in the field of advanced therapies, as reported by the EMA guidelines (Reflection paper on stem cell-based medicinal product, march 16, 2010), are:

- "embryonic stem cells (HESCs) derived from blastocysts, can be maintained in culture in vitro as well as other cell lines. HESCs are pluripotent and have the ability to differentiate into virtually any cell type present in the human body. Can be characterized by a distinct set of markers to cell surface, as well as by genetic markers of pluripotency. HESCs, as implanted in a permissive host for teratoma, form benign tumors composed of various cell types derived from the three germ layers, endoderm, mesoderm and ectoderm. HESCs can differentiate in vitro using or external factors added to the culture medium or through genetic modification. However, the in vitro differentiation often generates cell populations with a variable degree of heterogeneity.

- adult stem cells or somatic cells including:

a) stem cells / hematopoietic progenitors (HSCs). HSCs are cells capable of giving rise to differentiated cells belonging to all hematopoietic lineage, myeloid and lymphoid, both in the hematopoietic marrow that in the thymus. In the adult, the HSCs are localized in the bone marrow and are located at a lower frequency in the form circulating in the peripheral blood. At low frequencies can also be found in other tissues (liver, spleen, and muscle) but their origin and relevance to normal hematopoiesis have not yet been fully clarified. HSCs are

mobilized from the blood compartment after intensive treatment with chemotherapy and / or growth factors. These stem cells are also found in the placenta and umbilical cord blood at birth, at concentrations similar to those in the bone marrow in the adult.

b) mesenchymal stem / stromal cells (MSCs). MSCs are cells that are primarily derived from the stroma of the bone marrow or adipose tissue. In addition, mscs have been isolated from several other tissues such as retina, liver, gastric epithelium, tendons, synovial membrane, placenta, and umbilical cord blood. They have the ability to differentiate the various lineages and can be induced to differentiate into osteogenic, chondrogenic and adipogenic. MSCs can differentiate in neurons, astrocytes, tenocytes and skeletal myocytes. They also have a specific immunophenotype, which allows to select them using the technique of facs.

c) tissue-specific progenitor cells. These are cells that have a more limited ability to differentiate and normally produce only one cell type or a few cell types that are specific to that tissue.

- Induced pluripotent stem cells (IPS) are artificially generated from stem cells. Are reprogrammed from somatic stem cells such as fibroblasts of the skin. Ips cells share many characteristics with hescs, have the capacity for self-renewal, and are pluripotent and form teratomas. IPS cells are increasingly generated from different types of mature cells. Their ability of differentiation appears to depend on cell type and age of the cells from which ips are reprogrammed. There is a gap in knowledge that should be dealt with in relation to the alteration of some signaling pathways, differences in gene expression and epigenetic control. These features can result in chimerism or malfunction of cells. "

Bone marrow derived mesenchymal stem cells (MSCs) are a very small portion of pluripotent cells situated in the bone marrow. Mesenchymal stem cells can be isolated from a mixture of bone marrow cells on the basis of antibody expression selection procedures. The isolated msc can differentiate into numerous different cell types including the osteogenic lineage. Different

chemicals control differentiation into the osteoblastic phenotype, for example ascorbic acid, dexamethasone, and growth factors like BMPs, PDGF and TGF-β. One of the principal problems is the relative low MSCs concentration in the bone marrow. To obtain relevant amounts of cells, the cells have to be cultured and amplified ex vivo. During an extended ex vivo cultivation mesenchymal stem cells lose some of their phenotypic characteristics such as bone forming capability. [68, 69] Another drawback is the need of adequate sterilization of the cell-seeded scaffold before surgery. It has been be reported that scaffolds seeded with mscs have a better osteogenic capacity and show a faster integration with native tissue than acellular scaffolds. [70] The osteoinductive and osteogenetic properties of MSCs were demonstrated in several preclinical animal models treating critical sized bone defects with msc seeded matrices in different animals. [71, 72] Other studies reported the importance of the scaffold material on the properties of the inserted MSCs. For example MSCs on polycarbonates containing 0% or 3% of PEG up regulate the expression of estrogenic markers at different stages. Cells on polycarbonates containing no PEG were characterized as having early onset of cell spreading and osteogenic differentiation. Cells on 3% peg surfaces were delayed in cell spreading and osteogenic differentiation, but had the highest motility. [73]

Bioreactors

In the overall cell-based bone tissue-engineering strategy of expanding, culturing and differentiating stem cells on a three-dimensional scaffold to implant the scaffold in vivo, bioreactor can be used to enhance in vitro culture steps.

Bioreactor is an innovative method for in vitro cell culture that allows reaching a good level of production quality, standardizing the process, under controlled conditions as established by regulatory requirements.

Bioreactors utilize cells and materials that have previously been proven effective for bone tissue engineering, such as polymeric scaffolds and mesenchymal stem cells (MSCs). [74] [75] This population represents only a small percentage of cells found in the bone marrow, thus expanding these cells to clinically relevant numbers represents a significant problem to the implementation of a tissue engineering strategy. In addition to a readily available cell source, the use of bioabsorbable scaffolds is also important because ideally scaffolds degrade in vivo and are replaced by new bone tissue.

The cells expansion process is usually constituted by an open system that uses flasks or plates. This method requires frequent manual intervention, resulting in a potential risk of contamination. Crops standard "open" are more costly in terms of time needed for the growth and amplification of cellular also require expensive facilities. [76]

Bioreactors are tools created for fermentation and culture of bacteria and, successively, have been applied to tissue engineering. [77] Their aim is to recreate in vitro conditions typical of the biological environment present within the body, allowing the control of chemical-physical and mechanical parameters that influence the state, such as the pH, the concentration of gases (oxygen and carbon dioxide), the humidity and the temperature. Furthermore, bioreactors allow the physical and mechanical stimulation of the tissue construct during the culture phase. [78] A common feature of these devices is the capacity to generate flow pattern in the

culture medium, by establishing convective motions. This consent cells perfusion. Contrarily from what happens in static cultures in which everything is entrusted to the simple diffusion, in bioreactor the cells are better reached by nutrients and there is a more rapid removal of waste metabolites.

It was reported that bioreactors improve cell seeding efficiency, [79] [80] cells proliferation, [81] [82] and mesenchymal stem cell osteoblastic differentiation. [83]

The most significant contribution of bioreactor systems to a bone tissue engineering strategy is the possibility of automation.

In fact, automation is important to minimize the risk of contamination from bacteria and other cells, to reduce work amount, and to reduce costs associated with in vitro cell culture. Bioreactor systems have the potential to minimize all of these aspects through automated cell culture. A cell source could be added to a bioreactor, seeded using the bioreactor, and cultured continuously in a closed system. Nutrient and oxygen concentrations could be monitored by the system and media changes could be automated. Reducing the potential risk of contamination and work amount, bioreactors could improve the feasibility of bone tissue engineering strategies.

In the design of a bioreactor, there are some basic technical specifications that must be considered:

- all components of the device in contact with the culture should be sterilized or disposable and sterility absolutely maintained;
- the number and complexity of the steps for assembly or disassembly should be limited;

The bioreactors could be computer controlled to minimize or completely remove the need for operator intervention. [76]

Nursery of cell growth, which controls inoculation and cultivation of cells, can be connected to a memory device. In addition, there may be sensors of incoming and outgoing from the room,

to measure various parameters such as, the pH, the concentration of carbon dioxide, glucose, temperature etc.. All obtained data are stored by the memory device going to be part of the documentation to meet the requirements for operating accordingly to the standards of good manufacturing practice. [76] Again, completely closed systems remove most of the issues related to microbial contamination, which represent one of the major risks of using cells. [84]

In addition to the possibility of automation, bioreactors can improve in vitro cell culture especially in three-dimensional scaffolds. In fact, in these scaffolds, nutrient gradients develop in static culture where the cells at the surface are consuming oxygen, glucose, and other nutrients creating a gradient where cells nearer to the surface of the scaffold receive adequate nutrients, but the concentration of these nutrients decrease toward the center of the scaffold. If nutrient and oxygen concentrations drop below the minimum necessary to sustain cell growth, at the center of the scaffold cell death occurs. [85] This is empathized in bone tissue scaffold in which cells are producing matrix and this gradient is magnified as the matrix produced by cells on the exterior portion of the scaffold reduces nutrient transmission. To mitigate this bioreactor systems have been developed to optimize this process through dynamic culture and a controlled environment. Bioreactors that have been widely utilized in bone tissue engineering are: spinner flasks [86] [87], rotating wall [86] [88], and perfusion systems [89] [90]. These bioreactor types showed to be an effective means to culture cells for bone tissue engineering purposes. Spinner flask and rotating wall bioreactor systems are efficient to create a homogenous media solution on the exterior of the scaffold but do not effectively perfuse media inside. Perfusion systems have been demonstrated to effectively perfuse media throughout the scaffold and have been shown to upregulate osteoblastic markers and increase calcium deposition. Bioreactor systems, in particular perfusion systems, increase nutrient transport and expose cells to fluid shear stresses. An important feature of bioreactor systems is their ability to create an in vitro environment that is similar to the in

vivo environment of bone. [91] Although bioreactor systems cannot reproduce bone tissue environment, mechanical stresses and improved nutrient transport aid in enhancing in vitro cell culture. For example, limited transport of nutrients in static culture is in contrast to the in vivo conditions of bone that is a well-vascularized tissue. Bioreactor systems overcome these barriers via dynamic culture that improves nutrients transport and exposes cells to mechanical stress. Mechanical stimulation through fluid shear stresses has been shown to be important in bone differentiation and mineralization. [91] [92] Bone tissue constantly remodels itself in response to mechanical stresses. Some authors hypothesized that in vivo, these stresses are mainly transmitted to bone cells via fluid shear stresses. [93] As load is applied to bone, interstitial fluid flows through pores in the bone, and the shear stress is sensed by terminally differentiated osteoblasts known as osteocytes. The matrix network around these osteocytes may allow for communication with osteoblasts and osteoprogenitor cells. It is assessed that in response to loading, bone cells experience in vivo shears from 8 to 30 dyn/cm^2. [94] Osteoblasts and mesenchymal stem cells have also been shown to directly respond to shear stress. [90] [95]

A simple bioreactor system to achieve thorough media mixing is the spinner flask. Spinner flasks are composed of a glass media reservoir with side arms that can be opened to remove scaffolds and media and often have porous covers to allow for gas exchange. The flask has a stir bar or other stirring mechanism that stirs the media in the flask. Scaffolds are typically suspended from the top of the flask using needles or thread. [96] [97]

Spinner flasks bioreactors are often used in bone tissue engineering. They increase the expression of early osteoblastic marker alkaline phosphatase (ALP), late osteoblastic marker osteocalcin (OC), and calcium deposition as compared to static culture and rotating wall bioreactors. [97] This effect is thought to result from the convective transport of nutrients to the surface of the scaffold in spinner flask culture in contrast to the purely diffusional

transport in static culture. This increases also oxygen concentrations throughout the scaffold. In static culture, we observe a nutrient concentration gradient where cells in the center of the scaffold receive an insufficient supply of nutrients. [84] A nutrient gradient may still exist in spinner flask culture due to matrix deposition on the exterior portions of the scaffold. [97]

Some studies reported that spinner flask culture does not adequately increase mass transport and a sharp nutrient gradient results leading to cell death in the center of the scaffold. Penetration depth of transport in spinner flasks appeared to be limited to 1.0 mm or less. Despite these data, spinner flasks expose cells at the surface of scaffold to shear stress, which could aid in enhancing osteogenic differentiation. [82]

The differences in proliferation and differentiation observed between spinner flask and static culture could be caused by increased nutrient transfer or exposure to shear stresses. Culture conditions of spinner flask systems affect stem cell differentiation and proliferation. [98]

Another system used in bone tissue engineering to increase media mixing is the rotating wall bioreactor. The design features two concentric cylinders, an inner cylinder that is stationary and provides for gas exchange and an outer cylinder that rotates. [84] The space between the two cylinders is completely filled with culture media and cells enriched scaffolds are placed freely moving in this space. The free movement of the scaffolds leads to a microgravity environment however the flow of the fluid produced by the centrifugal forces of the cylinder balances with the force of gravity. [96] [97]

A slight variant of the rotating wall bioreactor is used in the rotational oxygen-permeable bioreactor system (ROBS) where scaffolds are cultured in a 50-ml polypropylene centrifuge tube modified with a silicone elastomer to provide for gas exchange. [99] The tubes containing the constructs are then placed on a roller device and housed in an incubator. This system provides both for gas exchange and rotational shear forces and was efficaciously used to culture BMSCs on polycaprolactone scaffolds. [100, 101]

Another slight variation of the traditional rotating wall bioreactor is that in which scaffolds are fixed to the vessel wall rather than allowed to move freely. [102]

Most of these bioreactors are uni-axial in design, which may place a constraint on the homogenous flow pattern of media. Some authors developed a biaxial rotating bioretactor, which incorporates a biaxial rotating wall vessel design with a media perfusion system in order to overcome the limit of uni-axial design. Under in-silico simulation this bioreactor demonstrated enhanced flow dynamic over uniaxial rotation. [103] [88]

Several studies comparing rotating wall bioreactors to static and spinner flask culture have been completed and reported less encouraging results for rotating wall bioreactors. [96] [104]

Perfusion bioreactors use a pump system to perfuse media directly through a scaffold. Many different perfusion bioreactor systems have been developed but most systems consist of a similar basic design containing of a media reservoir, a tubing circuit, a pump, and a perfusion cartridge. [91] The perfusion cartridge houses the scaffold, which is sealed so that media cannot flow around it. Consequently perfusion of media takes place directly through the pores of the scaffold. This direct perfusion makes these systems difficult to develop, as the perfusion cartridge must be custom made to closely fit a scaffold. The scaffold must have also highly interconnected pores. Despite these difficulties, many perfusion bioreactor systems have been developed and studied for bone tissue engineering purposes. [81] [82] [105] [92]

Most common in the literature is the flow perfusion culture bioreactor, that utilizes two media reservoirs to allow for complete media changes and a cassette that contains a scaffold press fit between two o-rings. [92] [106]

Aims

The aims of the present study were to investigate the local tolerance and the osteointegration capacity of a new biodegradable composite scaffold consisting of polycaprolactone (PLC) and β-tricalcium phosphate (TCP) enriched or not with mesenchymal stem cells.

Experimental procedures

Animals and operations. In the first experiment we evaluated the in vivo local tolerance in 4 immunodeficient (NOD/SCID) mice (2 male and 2 female animals) implanting the scaffold material enriched or not of human stem cells (abm007f) expanded in vitro in bioreactor and using hydroxyapatite scaffold as control. The animals were premedicated and subsequently general anesthesia was induced with xylazine hydrochloride and ketamine HCl. In each animal 5 subcutaneous implants were done as follow:

1. Pellet pcl+βtcp (dipping)
2. Pellet pcl+ βtcp (dipping)+ human mscs
3. Pellet pcl (no dipping)
4. Pellet pcl (no dipping)+ human mscs
5. Hydroxyapatite

Animals were sacrificed for histological examination at 4 weeks.

In the second step we assessed local tolerance and ectopic bone formation in 8 immunodeficient (NOD/SCID) mice (4 male and 4 female animals) in which we used the scaffold enriched or not of sheep stem cells obtained from bone marrow, expanded in vitro in bioreactor, and a hydroxyapatite scaffold as control. The animals were pre-medicated and subsequently general anesthesia was induced with xylazine hydrochloride and ketamine HCl in each animal 5 subcutaneous implants were done as follow:

1. Scaffold 3D pcl+βtcp (dipping)

2. Scaffold 3D pcl+ βtcp (dipping)+ sheep mscs

3. Scaffold 3D pcl (no dipping)

4. Scaffold 3D pcl (no dipping)+ sheep mscs

5. Hydroxyapatite.

Animals were sacrificed and histological evaluation was performed at 4 and 8 weeks from the implantation.

In the third experiment a rabbit model was used to evaluate osteointegration capability and local tolerance of this scaffold loaded or not of autologous stem cells obtained from bone marrow (expanded in vitro in bioreactor). The protocol consists of 5 experimental groups of animals (12 adult white New Zealand rabbits). For this, healthy and skeletally mature male New Zealand white rabbits were selected and cared according to guidelines for the care and use of laboratory animals. The animals were housed in individual cages.

Two weeks before surgery, a bone marrow sample was taken under general anesthesia. Bone marrow concentrate was successively processed and mesenchymal stem cells were isolated to be expanded in vitro in bioreactor. Surgery was performed under general anesthesia. The anesthesia was induced by an intramuscular injection of ketamine hydrochloride and 2% xylazine hydrochloride. The animals were placed in a ventral position for the insertion of the implants. Legs of the animals were shaved, washed, and disinfected with povidone–iodine. A midsagittal incision was made through the skin. The skin and subcutaneous tissue were separated from the periosteum by using blunt dissection. A second longitudinal incision was made through the periosteum, which was the elevated and care fully dissected from the underlying bone. After exposure, one full thickness bone defect (4 mm x 11 mm) was made in radial diaphysis. This kind of lesion allows implantation of the scaffold without any stabilization procedure due to intrinsic stability provided by the ulna. Subsequently, the

samples were inserted into the defects randomly. After inserting the scaffold, the skin was closed.

In detail:

1. In the first group 3 rabbits were treated with cellularised 3D samples (scaffold + dipping).
2. In the second group 3 rabbits were treated with not cellularised 3D samples (scaffold + dipping).
3. In the third group 3 rabbits were treated with the control material (hydroxyapatite).
4. The fourth group consisted of 2 animals treated with 3D scaffolds not cellularised and without dipping.
5. The fifth group consisted of a single animal without any implant.

Conventional x-rays were performed post-surgery and at weeks 4-8-12. Newly formed bone and callus formation in the defect area were characterized qualitatively. At 4, 8, and 12 weeks post-implantation, euthanasia was performed with tanax ev. after deep sedation, induced by combination of ketamine and xylazine. For histological study, the implants with surrounding bone tissue were removed, fixed with 4% formaldehyde in pbs, and then decalcified in 10% formic acid. After dehydration in a graded series of ethanol, the specimens were embedded in paraffin wax and cut into 5 mm transverse sections in the center of the bony defects. These sections were stained with hematoxyline and eosin for the observation by light microscopy.

In the last experiment we evaluated osteointegration and local tolerance of this scaffold enriched or not of autologous stems cells (expanded in vitro in bioreactor) in sheep. The protocol consist of 2 groups of 6 experimental animals each one. Two weeks before surgery, a bone marrow sample from iliac crest was taken, always under general anesthesia. Bone marrow concentrate was successively processed and mesenchymal stem cells were isolated to be expanded in vitro in bioreactor. In the first group we implanted 6 scaffolds in the tibial diaphysis and 2 scaffolds in the distal femoral epiphysis in the right leg and the control

material (hydroxyapatite) in the contra-lateral leg. In the second group we implanted with the same pattern of positioning the scaffolds and the hydroxyapatite enriched of autologous mesenchymal stem cells previously expanded in vitro in bioreactor. The animals were pre-medicated and subsequently general anesthesia was induced with xylazine hydrochloride and ketamine HCl during surgery, a bone defect of about 12mm x 5 mm was created before implantation as follows. The animals were placed in a lateral decubitus position for the insertion of the implants. Legs of the animals were shaved, washed, and disinfected with povidone–iodine. A mid-sagittal incision was made through the skin on the medial tibial diaphysis and an oblique skin incision was made on the lateral aspect of distal epiphysis of femur (knee). The skin and subcutaneous tissue were separated from the periosteum by using blunt dissection. A second longitudinal incision was made through the periosteum, which was the elevated and care fully dissected from the underlying bone. After exposure, full thickness bone defects were made in tibia and femur. This kind of lesion allows implantation of the scaffold without any stabilization procedure due to intrinsic stability (see fig. 1).

Subsequently, the samples were inserted into the defects randomly. After inserting the scaffold, the skin was closed.

Each group was divided in 3 subgroups in relation of experimental time of 6 weeks (2 animals), 12 weeks (2 animals), 24 weeks (2 animals). Bone growth and local tolerance were assessed histologically, radiographically and by micro-ct. Conventional x-rays were performed post-surgery and at weeks 6-12-24. Newly formed bone and callus formation in the defect area were characterized qualitatively. Micro-CT was employed to evaluate volumetric quantitative new bone formation.

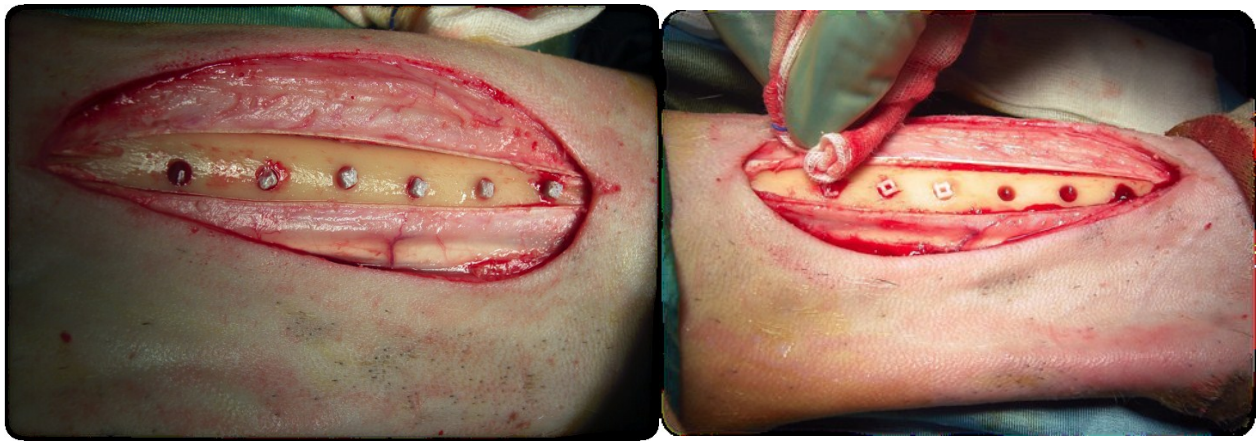

Fig. 1: implants of scaffolds and ceramic control materials in sheep (tibial diaphysis)

Results

In the first experiment in 4 immunodeficient (nod/scid) mice none of the sample induced even a minimal inflammatory reaction (see table 1).

Only a minimal lympho-monocyte infiltration was found in one of the ceramic samples used as control. Histological images with more detailed information for degradable scaffold materials were displayed in fig. 2 without obvious inflammatory reactions.

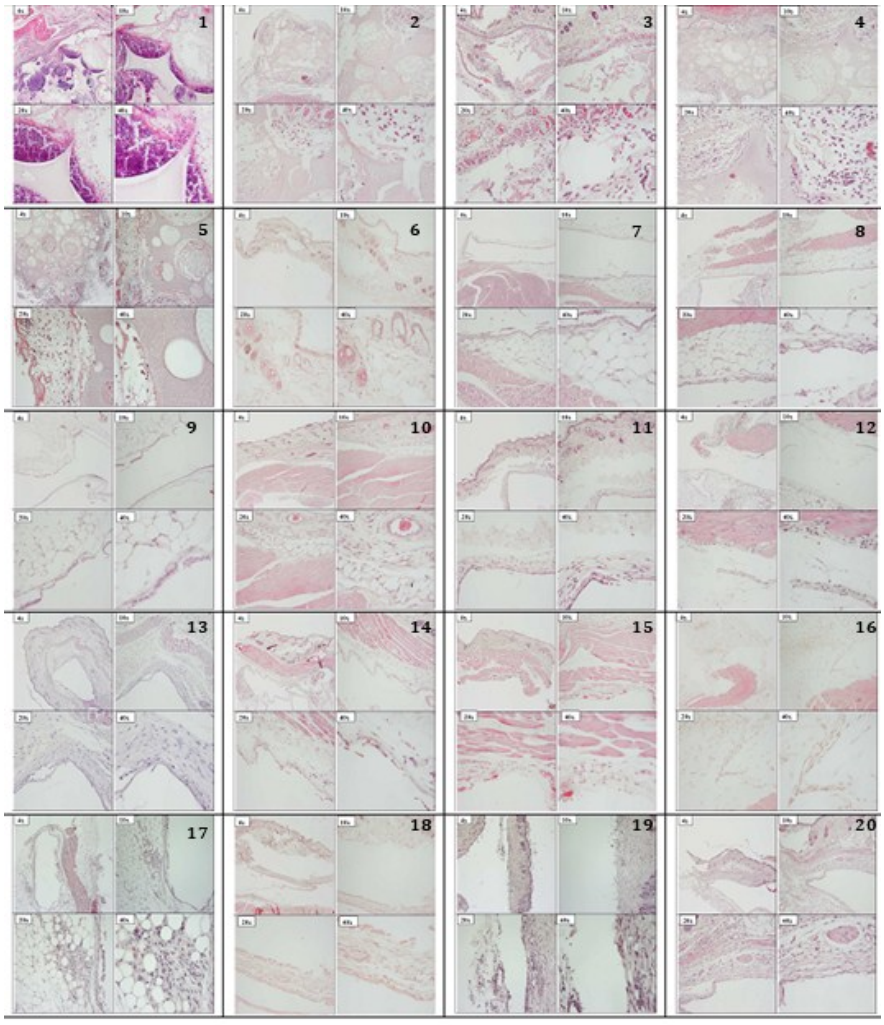

Figure 2: histological evaluation (photomicrographs): a minimal lympho-monocyte infiltration in one of the ceramic samples

Legend:

1→ example of inflammatory reaction: leukocyte infiltration

2,3,4,5 → (ha)ceramic material as control

6,7,8,9 → samples of polycaprolactone (pellet)

10,11,12,13 → samples of polycaprolactone (pellet) + hmscs

14,15,16,17 → samples of polycaprolactone (pellet) + dipping

18, 19, 20 → samples of polycaprolactone (pellet) + dipping + hmscs

Sample	*Male mouse 1*	*Male mouse 2*	*Female mouse 1*	*Female mouse 2*
Ha ctrl	-	-	+/-	-
P	-	-	-	-
Pc	-	-	-	-
Pd	-	-	-	-
Pdc	-	-	-	-

Tab. 1 Summary of inflammatory reaction in all samples

Legend:
p→ polycaprolactone pellet,
pc → polycaprolactone pellet + cells (hmscs),
pd→ polycaprolactone pellet + tcp,
pdc→ pd + cells (hmscs)

In the second experiment, as explained in experimental procedures paragraph, we assessed local tollerance and ectopic bone formation in 8 immunodeficient (nod/scid) mice. At 4 weeks all samples appear to be well integrated with the surrounding tissues. All the empty spaces of scaffolds are colonized by host tissue (fig. 3). All samples shown good vascularization (presence of both relatively large caliber vessels and capillaries) as summarized in table 2.

In macroscopic analysis we have not found evidence of infectious processes or inflammatory reaction.

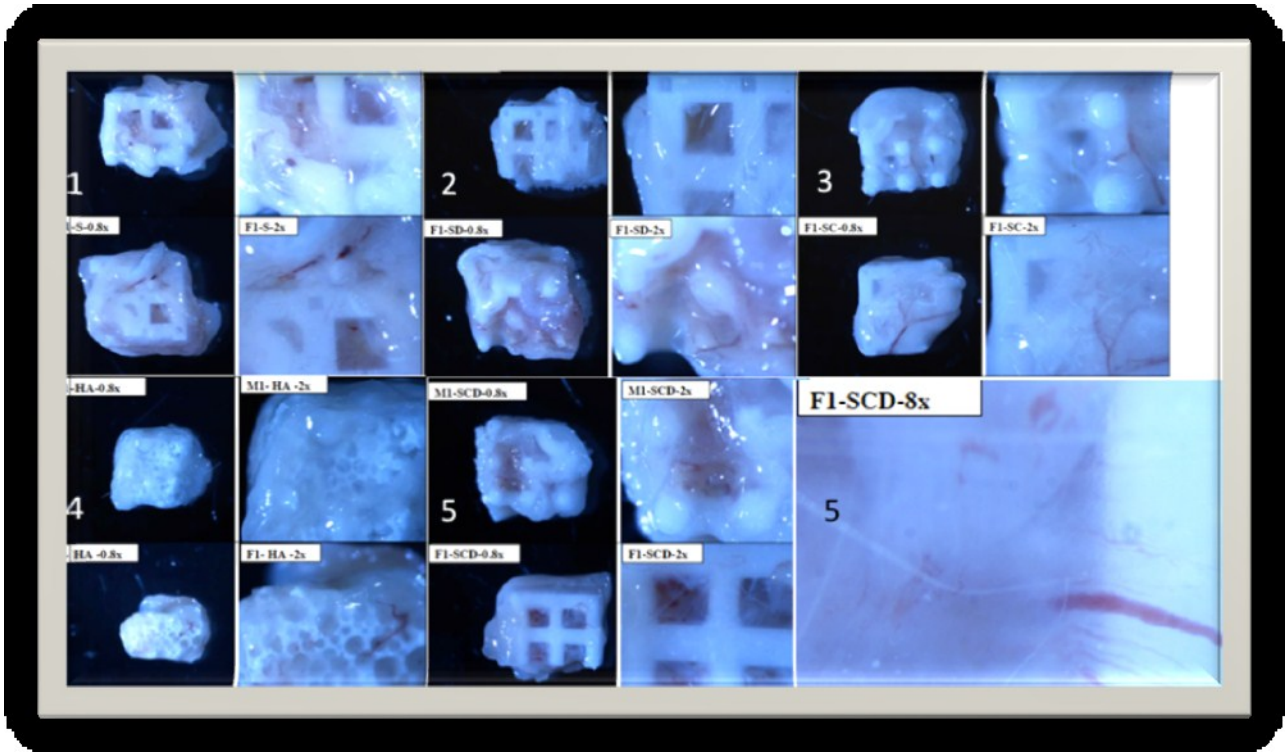

Fig. 3 Macroscopic evaluation of explanted samples showing good integration and vascular invasion of the empty space of samples

Legend:
1 → scaffold pcl +tcp
2 → scaffold pcl +tcp + dipping
3 → scaffold pcl +tcp + sheep mscs
4 → HA(ceramic material as control)
5,6 → scaffold pcl +tcp + dipping + sheep mscs

Sample	Mouse 1 male	Mouse 2 male	Mouse 1 female	Mouse 2 female
	Integr/vasc	Integr/vasc	Integr/vasc	Integr/vasc
Ha ctrl	+/+	+/+	+/+	+/+
S	+/+	+/+	+/+ exp*	+/+
Sd	+/+ exp*	+/+	+/+	+/+
Sc	+/+	+/+	+/+	+/+ exp*
Sdc	+/+ exp*	+/+ exp*	+/+	+/+

*exp → partially exposed sample, healed skin

Tab. 2 Macroscopic evidence of new bone formation and vascular invasion at 4 weeks after subcutaneous implantation of 3d scaffolds.

Histological evaluation

8 weeks after implantation the 3D explanted samples appeared to be well integrated with the surrounding tissues. All the empty spaces of the 3D samples are colonized by host tissue. All samples are well vascularized (presence of both, large vessels and capillaries). The SCD samples shown evidence of bone formation as summarized in table 3. At microscopic analysis there was no evidence of infectious processes or inflammatory reaction.

Sample	Mouse 1 male	Mouse 2 male	Mouse 1 female	Mouse 2 female
	Neoformation bone tissue	Neoformation bone tissue	Neoformation bone tissue	Neoformation bone tissue
Ha ctrl	-/-	-/-	-/-	-/-
S	-/-	-/-	-/-	-/-
Sd	-/-	-/- exp*	-/- exp*	-/-
Sc	-/-	-/-	-/-	-/-
Sdc	+/+ exp*	+/+	-/-	+/+

*exp → partially exposed sample, healed skin
Tab. 3 Microscopic evidence of new bone formation and vascular invasion at 8 weeks after subcutaneous implantation of 3d scaffolds.

A rabbit model, as described previously, was used to evaluate local tolerance and osteointegration of the scaffold. The scaffolds with and without cells were implanted into radial diaphysis defects of rabbits. During the experiment, all rabbits remained in good health and did not show any wound complications.

Radiological evaluation of implants in adult New Zealand white rabbits at 4, 8 and 12 weeks shown bone callus formation in all animals at 4 and 8 weeks, while defect healing has been obtained in the animals treated with scaffold or ceramic control (HA). In non-treated rabbit at 12 weeks is still identified a small bone defect. At explantation, no inflammatory signs or adverse tissue reaction were seen. All samples appeared well integrated with the surrounding tissues. Analysis of the scaffold sections via light microscopy revealed good osteointegration with various levels of bone formation at 8, and 12 weeks post-implantation in each group (see fig. 4). Moreover, throughout the observation periods, no lympho-monocytes infiltration was observed in all specimens and all empty spaces of scaffold have been filled by host tissue.

Results are summarized in table 4.

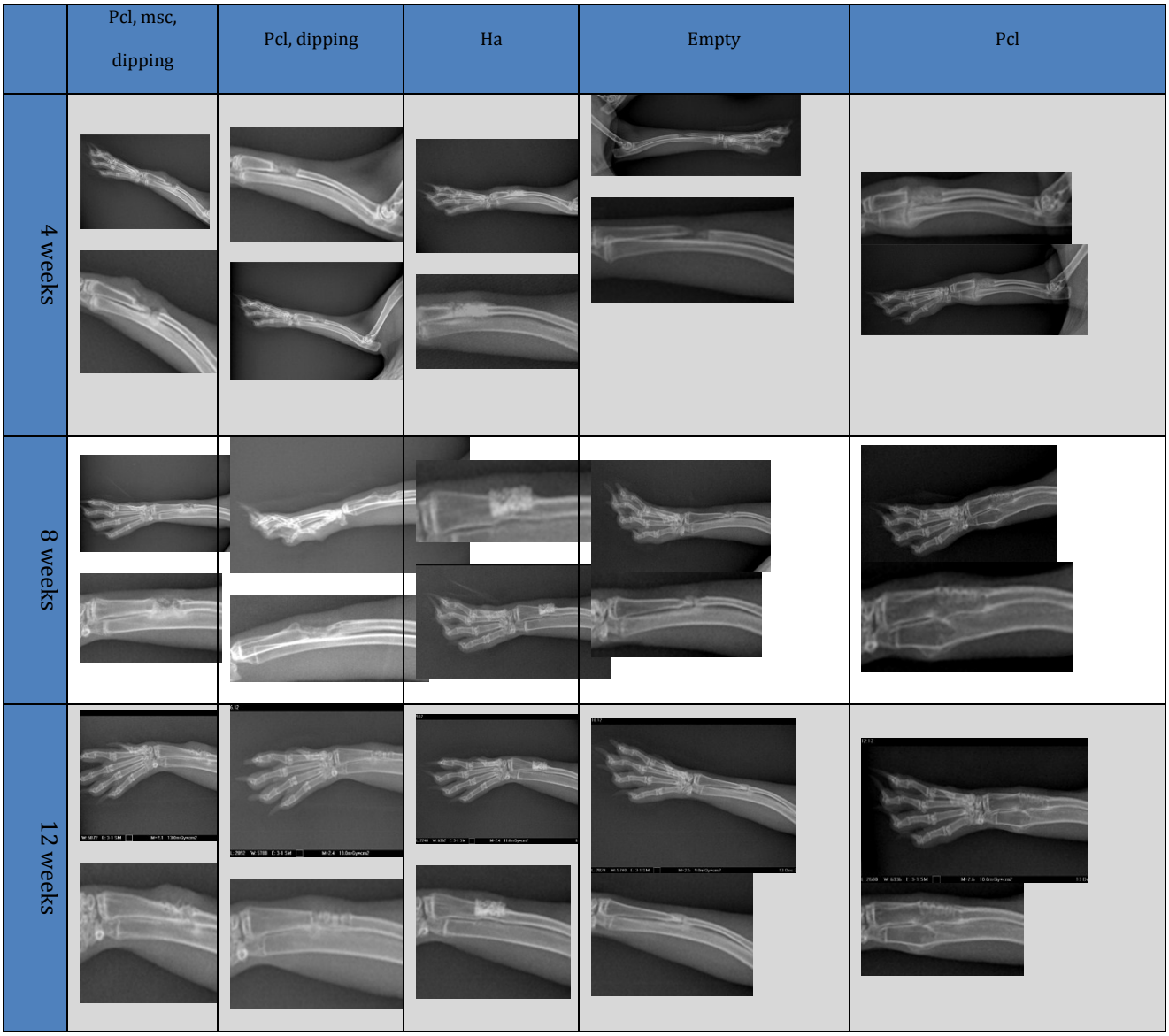

Fig. 4: x-ray evaluation at 4-8-12 weeks

	Rabbit number	Rb1	Rb2	Rb3	Rb4	Rb5	Rb6	Rb7	Rb8	Rb9	Rb10	Rb11	Rb12
	Sample implanted	Sdc	Sdc	Sdc	Sd	Sd	Sd	Ha	Ha	Ha	Mock/empty	Pcl	Pcl
3 w	Inflamm.	-	-	-	-	-	-	-	-	-	-	-	-
	Bone histo	+			+				+				
	Bone x-ray	+-	+-	+	+	+-	+-	+	+	+-	+-	+-	+
	Integr. Histo	+			+				+				
	Integr. X-ray	-	-	+-	+-	+	+-	+-	+	+-	**N/a**	+-	+-
	Cont. Bone histo	-			-				+-				
	Cont. Bone x-ray	-	-	+-	+-	+-	-	+-	+-	+-	-	-	-
	Central bone	+			-				+-				
8 w	Inflamm.		-	-		-	-	-		-	-	-	-
	Bone histo		+			+		+				+	
	Bone x-ray		+	+		+	+	+		+	+	+	+
	Integr. Histo		+			+-		+				+	
	Integr. X-ray		+-	+		+	+	+		+	**N/a**	+	+
	Cont. Bone histo		+-			+-		+-				+-	
	Cont. Bone x-ray		+-	+		+	+-	+		+	-	+	+
	Central bone		+			-		-				+	
12 w	Inflamm.			-			-			-	-		-
	Bone histo			++			++			++	++		++
	Bone x-ray			+			+			+	+		+
	Integr. Histo			++			++			++	**N/a**		++
	Integr. X-ray			+			+			+	**N/a**		+
	Cont. Bone histo			+			+			++	+		+-
	Cont. Bone x-ray			+			+			+	+-		+
	Central bone			++			++			++	+-		+

Tab. 4 Summary of the radiological and histological evaluation in rabbit model

Legend:

Inflamm.	Macroscopic or microscopic signs of inflammation (redness, swelling, lymphocytic infiltrate etc.)
Bone histo	Assessment of bone tissue presence in microscopic fields analyzed
Bone x-ray	Radio-opacity evaluation
Integr. Histo	Histological evaluation of bone stumps and implanted materials integration
Integr. X-ray	Radiographic evaluation of bone stumps and implanted materials integration
Cont. Bone histo	Histological evaluation of bone tissue continuity along the implant area
Cont. Bone x-ray	Radiographic evaluation of bone tissue continuity along the implant area
Central bone	Presence of bone in the implant central area

In the last experiment a sheep model, as described previously, was used to evaluate local tolerance and osteointegration of the scaffold. Conventional x-ray evaluation of the implants, with details of tibial diaphysis and femoral condyles, showed at 6 weeks after surgery implants clearly visible in tibia, in particular for the hydroxyapatite implants. No signs of osteolysis were found. In the femoral lateral condyles samples of hydroxyapatite with or without mesenchymal stem cells are not visible due to their small size and their intrinsic radiopacity similar to trabecular bone. On the other hand, PCL/TCP samples without mesenchymal stem cells are visible in the implant site in 2 specimens and not visible in implant site the cells seeded PCL/TCP scaffolds. Otherwise, there was no evidence of osteolysis in all specimens.

The micro-ct results at six weeks are shown in table 5.

	Mean of ha samples (n.6) in cortical bone tissue	Mean of pcl/tcp samples (n.6) in cortical bone tissue	Mean of ha samples (n.2) in trabecular bone tissue	Mean of pcl/tcp samples (n.2) in trabecular bone tissue	Mean of ha + bmsc samples (n.6) in cortical bone tissue	Mean of pcl/tcp + bmsc samples (n.6) in cortical bone tissue	Mean of ha samples + bmsc (n.2) in trabecular bone tissue	Mean of pcl/tcp + bmsc samples (n.2) in trabecular bone tissue
Mat.v/tv	22,29 ±5,04		31,05±11,40		22,03±3,46		37,70±6,80	
Mat. Fr.i	5,69±1,25		-1,24±4,59		3,31±1,62		-2,24±2,28	
Bv/tv	27,91±2,06	18,39±2,00	15,33±1,19	4,24±0,70	24,45±2,33	17,78±3,64	14,99±1,92	5,03±2,14

Tab.5 Micro-ct results at 6 weeks after implantation.

Legend:

-mat.v/tv (%): percentage of material in the bone defect expressed as the ratio between the volume of the material present in the defect and the total volume of the bone defect. Calculated only in the samples implanted with ha because the implant of pcl/tcp does not appear to have sufficient contrast for images segmentation.
- mat fr.i (in mm-1): index of fragmentation of the implant material. A lower value of this index represents a greater connection of the material inside the defect, while a higher value of mat fr.i represents a material structure disconnected and fragmented inside the defect. also this parameter was calculated only in the samples of ha.
- bv / tv (in%): bone density expressed as the ratio between the volume of new bone inside of the bone defect and the total volume of the defect. This ratio was calculated in all samples.

Histological and histomorphometric analysis were performed in 3 samples from tibia (cortical bone) and 1 from femur (trabecular bone) for each material and animal in the group without stem cells and in one animal of the msc enriched group, while in one sheep of msc group was performed histological evaluation in 6 samples implanted in cortical bone and in 2 sample implanted in trabecular bone for each material. Results are shown in table 6.

Parameters	Samples	Tibia	Femur	Tibia	Femur
Mar (µm/day)	PCL/TCP	2,2±0,5	1,7	2,3±0,5	-
	Ha	2,0±0,8	5,1	3,6±1,5	2,8
	PCL/TCP +bmsc	1,7±0,4	2,21/1,87	1,7±0,8	0,93/1,67
	Ha + bmsc	1,5±0,5	1,57/1,57	1,9±0,7	0,83/1,33
Bfr (µm²/µm/day)	PCL/TCP	1,7±0,1	1,6	1,4±0,5	-
	Ha	2,0±0,8	4,0	3,7±1,9	1,3
	PCL/TCP +bmsc	1,6±0,6	1,93/1,21	1,3±0,7	1,71/0,83
	Ha + bmsc	1,5±0,1	1,22/1,17	1,7±0,3	1,71/0,83

Tab. 6 Histomorphometry of samples expianted at 6 weeks

Legend:
mar →mineral apposition rate. Mineralization rate of newly formed bone calculated as the ratio between the distance between two bands of fluorescence of a same trabecula divided by the number of days between the first and second marking.
Bfr →bone formation rate: rate of bone formation expressed as amount of newly formed bone mineralized (area) on the front of growth of bone trabeculae (perimeter) per unit time (day) by applying the following formula: mar * (1/2 sl.pm / b.pm + dl.pm / b.pm).

At 12 weeks x-ray evaluation of the second group (with and without msc) of sheeps was done. Analyzing tibial diaphysis and femoral condyles, the implants are clearly visible at the level tibial (preferably those of hydroxyapatite) and there were no signs of osteolysis.

In the lateral femoral condyles are not visible nor the implantation sites of the samples of hydroxyapatite nor those of PCL/TCP.

In all cases there was no evidence of osteolysis. As in the previous step (6 weeks) micro-CT evaluation was performed on 3 samples implanted in cortical bone and 1 sample implanted in trabecular bone for material and animal. The micro-CT results at 12 weeks are shown in table 7.

	Mean of ha samples (n.6) in cortical bone tissue	Mean of pcl/tcp samples (n.6) in cortical bone tissue	Mean of ha samples (n.1) in trabecular bone tissue	Mean of pcl/tcp samples (n.2) in trabecular bone tissue	Mean of ha + bmsc samples (n.6) in cortical bone tissue	Mean of pcl/tcp + bmsc samples (n.6) in cortical bone tissue	Mean of ha samples + bmsc (n.2) in trabecular bone tissue	Mean of pcl/tcp + bmsc samples (n.2) in trabecular bone tissue
Mat.v/tv	15,33 ±3,90		14,35		20,98±10,32		27,39±7,57	
Mat. Fr.i	9,48±3,96		1,26		8,49±3,08		4,18±4,04	
Bv/tv	47,10±7,47	34,36±2,81	11,06	13,29±1,58	43,93±6,14	47,82±1,94	19,50±0,90	4,74±1,79

Tab. 7 Micro-ct results at 12 weeks after implantation. Index and ratio are expressed as m value ± standard deviation

Legend:

-mat.v/tv (%): percentage of material in the bone defect expressed as the ratio between the volume of the material present in the defect and the total volume of the bone defect. Calculated only in the samples implanted with ha because the implant of pcl/tcp does not appear to have sufficient contrast for images segmentation.
- mat fr.i (in mm-1): index of fragmentation of the implant material. A lower value of this index represents a greater connection of the material inside the defect, while a higher value of mat fr.i represents a material structure disconnected and fragmented inside the defect. Also this parameter was calculated only in the samples of ha.
- bv / tv (in%): bone density expressed as the ratio between the volume of new bone inside of the bone defect and the total volume of the defect. This ratio was calculated in all samples.

Histological and histomorphometric analysis at 12 weeks from surgery were performed in 6 samples from tibia (cortical bone) and 2 from femur (trabecular bone) for each material and animal. Results are described in table 8.

Parameters	Samples	Tibia	Femur	Tibia	Femur
Mar (μm/day)	PCL/TCP	1,2±0,4	0,4/1,3	1,7±0,6	1,3/0,7
	Ha	1,3±0,2	1,3/1,2	1,4±0,2	-/-
	PCL/TCP +bmsc	1,5±0,3	1,4/0,8	1,5±0,5	2,7/1,1
	Ha + bmsc	1,5±0,4	0,7/1,3	1,8±0,4	1,6/1,4
Bfr ($\mu m^2/\mu m$/day)	PCL/TCP	1,0±0,1	0,4/0,9	1,4±0,1	1,3/0,8
	Ha	1,4±0,1	1,2/0,9	1,7±0,2	-/-
	PCL/TCP +bmsc	1,3±0,1	1,3/0,7	1,4±0,1	3,2/1,2
	Ha + bmsc	1,2±0,1	0,6/0,9	2,1±0,1	1,3/0,9

Tab. 8 Histomorphometry of samples expianted at 12 weeks: m.a.r. and b.f.r. expressed as value ± standard deviation

Legend:

mar →mineral apposition rate. Mineralization rate of newly formed bone calculated as the ratio between the distance between two bands of fluorescence of a same trabecula divided by the number of days between the first and second marking.

Bfr →bone formation rate: rate of bone formation expressed as amount of newly formed bone mineralized (area) on the front of growth of bone trabeculae (perimeter) per unit time (day) by applying the following formula: mar * (1/2 sl.pm / b.pm + dl.pm / b.pm).

Third group of specimens was explanted and analyzed at 24 weeks after surgery.

X-ray evaluation of samples (with and without msc) was done as in previous steps analyzing tibial diaphysis and femoral condyles.

The implants are clearly visible at level tibial (preferably those of hydroxyapatite) and there were no signs of osteolysis.

In the lateral femoral condyles are not visible nor the implantation sites of the samples of hydroxyapatite nor those of PCL/TCP. In all cases there was no evidence of osteolysis. Micro-ct evaluation a 24 weeks, as in previous steps, was performed on 3 samples implanted in cortical bone and 1 sample implanted in trabecular bone for each material and animal.

Results are described in table 9.

	Mean of ha samples (n.6) in cortical bone tissue	Mean of pcl/tcp samples (n.6) in cortical bone tissue	Mean of ha samples (n.2) in trabecular bone tissue	Mean of pcl/tcp samples (n.2) in trabecular bone tissue	Mean of ha + bmsc samples (n.6) in cortical bone tissue	Mean of pcl/tcp + bmsc samples (n.6) in cortical bone tissue	Mean of ha samples + bmsc (n.2) in trabecular bone tissue	Mean of pcl/tcp + bmsc samples (n.2) in trabecular bone tissue
Mat.v/tv	16,90 ±4,24		15,24±5,72		21,16±2,94		16,27±4,78	
Mat. Fr.i	17,01±3,20		7,99±2,19		14,02±3,34		7,11±2,63	
Bv/tv	55,33±4,69	41,56±3,23	26,35±0,10	12,13±1,36	46,87±6,26	42,30±3,66	34,38±6,02	24,47±19,54

Tab. 9 micro ct results at 24 weeks after implantation. Index and ratio are expressed as mean ± standard deviation

Legend:
-mat.v/tv (%): percentage of material in the bone defect expressed as the ratio between the volume of the material present in the defect and the total volume of the bone defect. Calculated only in the samples implanted with ha because the implant of pcl/tcp does not appear to have sufficient contrast for images segmentation.
- mat fr.i (in mm-1): index of fragmentation of the implant material. A lower value of this index represents a greater connection of the material inside the defect, while a higher value of mat fr.i represents a material structure disconnected and fragmented inside the defect. also this parameter was calculated only in the samples of ha.
- bv / tv (in%): bone density expressed as the ratio between the volume of new bone inside of the bone defect and the total volume of the defect. This ratio was calculated in all samples.

Data of histological and histomorphometric analysis at 24 weeks from surgery, performed in 6 samples from tibia (cortical bone) and 2 from femur (trabecular bone) for each material and animal, are shown in table 10.

Parameters	Samples	Tibia	Femur	Tibia	Femur
Mar (μm/day)	PCL/TCP	1,2±0,36	1,43/2,09	1,95±0,75	1,60/2,07
	Ha	2,24±0,46	1,44/1,86	2,65±0,79	2,62/1,95
	PCL/TCP +bmsc	1,82±0,97	4,33/4,17	2,99±1,38	-/-
	Ha + bmsc	3,09±1,42	3,87/2,96	2,77±0,79	-/-
Bfr (μm^2/μm/day)	PCL/TCP	0,91±0,31	1,60/2,07	1,23±0,53	0,73/1,33
	Ha	1,49±0,33	0,91/1,72	2,20±0,59	1,68/1,58
	PCL/TCP +bmsc	1,59±0,87	3,04/2,5	2,64±1,23	-/-
	Ha + bmsc	2,74±1,09	2,71/3,1	2,24±0,45	-/-

Tab. 10 histomorphometry of samples expianted at 24 weeks

Legend:
Mar →mineral apposition rate. Mineralization rate of newly formed bone calculated as the ratio between the distance between two bands of fluorescence of a same trabecula divided by the number of days between the first and second marking.
Bfr →bone formation rate: rate of bone formation expressed as amount of newly formed bone mineralized (area) on the front of growth of bone trabeculae (perimeter) per unit time (day) by applying the following formula: mar * (1/2 sl.pm / b.pm + dl.pm / b.pm).

Discussion

Over the last decades, research has advanced in many aspects of bone defects treatment, understanding the factors involved in bone healing process. So, currently, regenerative medicine gives to surgeons a variety of solutions such as scaffolds, powder, pastes and putty available in the market and approved as medical device for clinical use. Many studies have showed efficacious bone repair, but limited to repair of small bone defects, probably due to poor vascularization. Moreover, main issues of these scaffolds remain mechanical integrity and bioactivity. Some scaffolds are made with non-biodegradable materials, which are exposed to infection risk over long-term implantation. In bone regeneration structural properties for a three-dimensional bone scaffold, such as mechanical strength, pore size, porosity and interconnectivity between the pores play an essential role. [107] However, mechanical properties of a scaffold significantly depend on the architecture of the scaffold. Actually regarding bone regeneration, there is no consensus concerning the optimal scaffold design. It seems that the optimal pore sizes for bone ingrowth and regeneration is highly dependent of pore structures as well as scaffold materials used. In fact, some authors reported that the scaffolds with pore sizes larger than 150 μm were suitable for bone ingrowth [108], while other authors reported that bone formation and ingrowth occurred in scaffolds within 350 μm pore size, but the scaffolds with the pore size less than 200 μm had no bone ingrowth [47]. It was also reported that excellent bone ingrowth occurred in scaffolds with larger pore sizes than 400 μm [109].

The scaffold composite by PCL/TCP investigated in this study showed a good behavior in vivo. In fact, as already mentioned, none of the samples analyzed in this study induced even a minimal inflammatory reaction in mice, rabbit, and sheep models. Only a minimal lympho-monocyte infiltration in one of the HA samples (in mice) was found. This finding is occasional

and can be attributed to various causes not necessarily relater to the material used.
In mice, a good but uneven presence of newly bone formation has been found only in the samples enriched of mesenchymal stem cells. At 8 weeks after implantation, the presence of cuboidal osteoblasts on the newly bone tissue surface indicates a bone deposition process in the active phase. In the other samples presence of new bone tissue was not detected, while in many of such samples, a formation of fibrous tissue is shown that appear to coat the polymer. This evidence is consistent with the formation of a fibrous capsule.

On the other hand, in the porous ceramic samples, used ad controls, there was neither in vivo bone formation nor any fibrous capsule. In the rabbit model, new bone formation and good vascularization within the scaffold were observed in all samples studied. Interestingly, in the sample without stem cell histological examination has shown the presence of marrow cells within the scaffold. The sheep model, confirm absence of inflammatory reaction, good vascularization and improved bone ingrowth within the scaffold. In fact, micro-tomography evaluation showed in the bone defects trends for improved bone formation with the PCL/TCP and HA scaffolds either with o without BMSC. Furthermore, quantitative analysis of the histological sections taken (histomorphometric assessment) at the midpoint of the defect showed a trend for increased new bone formation as described in other studies with PCL [110]

In other studies, the PCL/TCP composite scaffold showed inferior behavior compared to other materials in a critical size defect [111] regarding promotion of bone regeneration, scaffold degradation and inflammatory reaction. [112] [113] The cause for the inflammation remained unclear. Due to the lower level of newly formed bone, PCL/TCP also led to a reduced biomechanical strength of the repaired bone.

In addition, in the present study, all the empty spaces of the 3d scaffold were colonized by host tissue and all samples appeared well vascularized with presence of both, large vessels and capillaries. Previous studies confirm these results reporting extensive vasculature formation within a PCL/TCP scaffold upon implantation with mesenchymal stem cells and platelet-enriched plasma. [114] In addition, the scaffold micro-architecture also plays an important role in supporting vascular formation and growth. There has been promising evidence showing ability of scaffolds in supporting vasculature formation within macro-porous scaffolds. Generally, a pore size of 150-500 μm is used in bone tissue scaffolds for supporting vascularization and blood vessels invasion. [52]

Conclusions

In the present study the bio-absorbable PCL/TCP scaffold enriched of autologous mesenchymal stem cells shows to promote new bone formation and to be well tolerated by host (no inflammatory reaction was observed). The results of this study suggest the PCL/TCP scaffold fabricated with peculiar design is safety and useful for recovering and enhancing new bone formation in bony defects in animals. More studies have to be done to confirm these results. In particular, there is still one more step to take: the human in vivo step.

Materials and methods

Scaffold characterization

The product VBC autologous bone small fragment (ASBF) is composed of a 3D biodegradable scaffold in polycaprolactone and β-tricalcium phosphate loaded with autologous osteoprogenitor cells, isolated from bone marrow and expanded in vitro with autologous serum, integrated in the same.

The materials used in manufacturing process are therefore two:

1 - cellular component: consisting of autologous mesenchymal stem cells isolated from autologous bone marrow

2 - scaffold: it consisting of a medical device in accordance with directive 93/42/ec, as amended by the recent Dir 2007/47/ec.

The scaffold consists of polycaprolactone, an aliphatic polyester already FDA-approved, used in similar applications, FDA approved.

The finished product consists of a small fragment consisting of autologous osteoprogenitor cells, expanded in vitro on a 3D scaffold, custom-made for each individual patient, for applications of orthopedic, oral-dental and maxillofacial surgery. In this way we obtain a highly personalized product, eliminating all possible risks from the use of allogeneic or xenogeneic cells or by immune reactions, the onset of inflammation and the risk of infections that can affect the entire outcome of the therapy.

Cellular component

The cells used are autologous mesenchymal stem cells from bone marrow, from the iliac crest of the animal. After withdrawal, the mononuclear cells are separated using centrifugation in a density gradient (ficoll) and then seeded on the scaffold, place inside a sterile chamber,

allocated in a bioreactor. The culture medium utilizes autologous serum, further reducing the risk of infection for the animal.

After 15 days of expansion, the fragment is removed to be implanted.

The scaffold

For the production of the scaffold 3 synthetic polymers were tested in order to identify the most suitable for the realization of the product: polyamide, polylactic acid and polycaprolactone. The final choice was in favor of polycaprolactone.

This is one of newly developed biomaterials that are most used in the field of tissue engineering. Initially used for the realization of degradable films and molds, today is widely used in various areas of biotechnology such as organ substitution, the realization of absorbable sutures, drug delivery for the controlled release of drugs, as well as, in recent years, the tissue engineering applied to the bone tissue. Polycaprolactone is a semi-crystalline polymer, aliphatic polyester synthetic, non-toxic, biodegradable and hydrophobic. In vivo is degraded by hydrolysis and, as the only metabolite, releases hydroxicapronic acid, product of non-enzymatic hydrolysis of ester, followed by fragmentation and release of oligomers. The latter are then digested by macrophages. To support these considerations, some studies [115] have shown that, following the process of degradation in vivo, this polymer secretes non-toxic products readily disposable by the body. The degradation time in a physiological environment, in contact with saline solutions of various natures is between three and twelve months.

Polycaprolactone also has the advantage of being able to be derivatized with other materials. Specifically, for the device VBC was chosen to produce a scaffold containing 80% of pcl and 20% of β-tricalcium phosphate (β -TCP), known for its osteoconductive characteristics.

Production of the scaffold

The technique used by VivaBioCell for the production of scaffolds, falls into the category of non-conventional techniques, the micro molding. This technique offers several advantages:

- provides solutions at a lower cost than other techniques,
- allows you to create structures with complex geometries,
- provides a process of manufacturing dimensionally stable,
- eliminates contamination from other particles,
- allows you to use alternative resins or fillers to improve the mechanical and / or electrical
- the surface is finished better.

Moreover, it allows to use as starting material the PCL with the TCP unlike other techniques, such as selective laser sintering, which does not allow to derivatize the PCL with the TCP. The scaffold is a lattice-like structure (see figure 5) held fixed inside the main chamber by a central, cylindrical hollow pipe, which fits onto a cylindrical support. The scaffold is made of square fibers arranged in a 5**x**5**x**5 matrix. The fiber interdistance is 1.25 times the fiber dimension. A free volume is available around the scaffold (1 mm thick) for fluid flow. (Campagnolo et al.)

The scaffold is obtained. It is an object of the cubic form of side 1 cm, 5 floors. Along the axis is housed the hollow cylindrical structure that serves as a site for placement of the screw which then, in vivo, in immobilize the site of implantation.

Bioreactor

The bioreactor allows to develop the process of cell expansion under standardized conditions, within a closed system and sterile, thus reducing to a minimum the intervention of the operator and therefore the risks related to processes of manufacture of this kind. The room in which is housed the scaffold with cells is a sterile disposable, as are all the components necessary to power the circuit for the expansion (tubes). The flow of the ground is closed, regulated by a pump, without parts, but the amount of the circulating medium is sufficient in order to allow cell proliferation within the limits set. Sensors for the control of various parameters such as pH, carbon dioxide, glucose etc., incoming and outgoing from the bedroom of culture, maintain the process control.

A sketch of the bioreactor and scaffold is shown in figure 5. The flow enters from the bottom side through a cylindrical pipe (feeding pipe) and is fed to the main chamber through four distributing pipes and a conical join (distributing cone). The bioreactor has been designed to feed continuously a water solution of glucose and oxygen to the cells initially seeded on scaffold walls. (Campagnolo et al.)

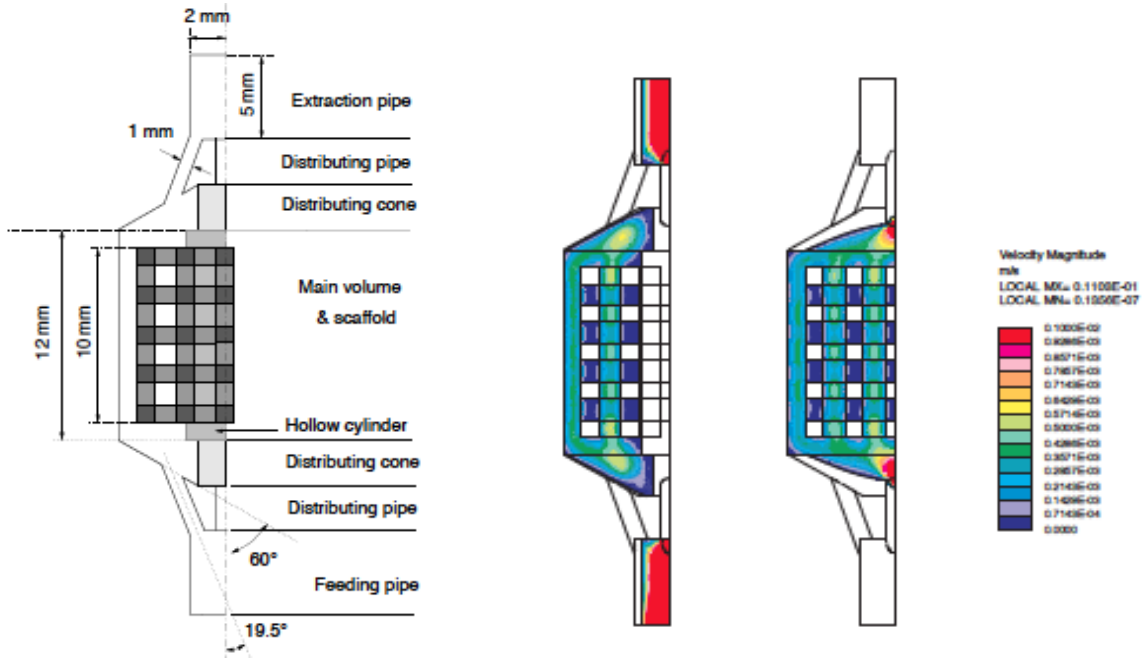

Fig. 5: sketch of the scaffold and bioreactor and flow velocity inside the scaffold. The flow follows a specific pattern, moving preferentially along main scaffold channels.

References

[1] Sullivan F. U.S. bone grafts and bone substitutes markets. 2007.
[2] Dawson JI, Oreffo RO. Bridging the regeneration gap: stem cells, biomaterials and clinical translation in bone tissue engineering. Archives of biochemistry and biophysics 2008;473:124-31.
[3] Reddi AH. Morphogenesis and tissue engineering of bone and cartilage: inductive signals, stem cells, and biomimetic biomaterials. Tissue engineering 2000;6:351-9.
[4] Vortkamp A, Pathi S, Peretti GM, Caruso EM, Zaleske DJ, Tabin CJ. Recapitulation of signals regulating embryonic bone formation during postnatal growth and in fracture repair. Mechanisms of development 1998;71:65-76.
[5] Einhorn TA. Breakout session. 1: Definitions of fracture repair. Clinical orthopaedics and related research 1998:S353.
[6] Johner R. [Dependence of bone healing on defect size]. Helvetica chirurgica acta 1972;39:409-11.
[7] Schenk RK, Willenegger HR. [Histology of primary bone healing: modifications and limits of recovery of gaps in relation to extent of the defect (author's transl)]. Unfallheilkunde 1977;80:155-60.
[8] Harris WH, White RE, Jr., McCarthy JC, Walker PS, Weinberg EH. Bony ingrowth fixation of the acetabular component in canine hip joint arthroplasty. Clinical orthopaedics and related research 1983:7-11.
[9] Browner B, D. Skeletal trauma: basic science, management, and reconstruction. 2003.
[10] Kujala S, Ryhanen J, Danilov A, Tuukkanen J. Effect of porosity on the osteointegration and bone ingrowth of a weight-bearing nickel-titanium bone graft substitute. Biomaterials 2003;24:4691-7.
[11] Hoshikawa A, Fukui N, Fukuda A, Sawamura T, Hattori M, Nakamura K, et al. Quantitative analysis of the resorption and osteoconduction process of a calcium phosphate cement and its mechanical effect for screw fixation. Biomaterials 2003;24:4967-75.
[12] Jukes JM, Both SK, Leusink A, Sterk LM, van Blitterswijk CA, de Boer J. Endochondral bone tissue engineering using embryonic stem cells. Proceedings of the National Academy of Sciences of the United States of America 2008;105:6840-5.
[13] Montjovent MO, Mark S, Mathieu L, Scaletta C, Scherberich A, Delabarde C, et al. Human fetal bone cells associated with ceramic reinforced PLA scaffolds for tissue engineering. Bone 2008;42:554-64.
[14] Tseng SS, Lee MA, Reddi AH. Nonunions and the potential of stem cells in fracture-healing. The Journal of bone and joint surgery American volume 2008;90 Suppl 1:92-8.
[15] Bose S, Roy M, Bandyopadhyay A. Recent advances in bone tissue engineering scaffolds. Trends in biotechnology 2012;30:546-54.
[16] Scaglione S, Giannoni P, Bianchini P, Sandri M, Marotta R, Firpo G, et al. Order versus Disorder: in vivo bone formation within osteoconductive scaffolds. Scientific reports 2012;2:274.
[17] Williams D. The relationship between biomaterials and nanotechnology. Biomaterials 2008;29:1737-8.
[18] Rouwkema J, Rivron NC, van Blitterswijk CA. Vascularization in tissue engineering. Trends in biotechnology 2008;26:434-41.
[19] Murphy CM, Haugh MG, O'Brien FJ. The effect of mean pore size on cell attachment, proliferation and migration in collagen-glycosaminoglycan scaffolds for bone tissue engineering. Biomaterials 2010;31:461-6.

[20] Woodard JR, Hilldore AJ, Lan SK, Park CJ, Morgan AW, Eurell JA, et al. The mechanical properties and osteoconductivity of hydroxyapatite bone scaffolds with multi-scale porosity. Biomaterials 2007;28:45-54.
[21] Rezwan K, Chen QZ, Blaker JJ, Boccaccini AR. Biodegradable and bioactive porous polymer/inorganic composite scaffolds for bone tissue engineering. Biomaterials 2006;27:3413-31.
[22] Williams DF. On the mechanisms of biocompatibility. Biomaterials 2008;29:2941-53.
[23] Lichte P, Pape HC, Pufe T, Kobbe P, Fischer H. Scaffolds for bone healing: concepts, materials and evidence. Injury 2011;42:569-73.
[24] Plannel J. Bone repair biomaterials. Cambridge UK 2009.
[25] Salgado AJ, Coutinho OP, Reis RL. Bone tissue engineering: state of the art and future trends. Macromolecular bioscience 2004;4:743-65.
[26] Lee SH, Shin H. Matrices and scaffolds for delivery of bioactive molecules in bone and cartilage tissue engineering. Advanced drug delivery reviews 2007;59:339-59.
[27] Lane JM, Tomin E, Bostrom MP. Biosynthetic bone grafting. Clinical orthopaedics and related research 1999:S107-17.
[28] Bostman OM, Laitinen OM, Tynninen O, Salminen ST, Pihlajamaki HK. Tissue restoration after resorption of polyglycolide and poly-laevo-lactic acid screws. The Journal of bone and joint surgery British volume 2005;87:1575-80.
[29] Cheung H-Y. A critical review on polymer-based bioengineered materials for scaffold development. Compos Part B;ENG 291-300.
[30] William d, Callister, j. Materials science and engineering: an introduction. . 2007 7th ed jhon wiley and sons.
[31] Balla VK, Bodhak S, Bose S, Bandyopadhyay A. Porous tantalum structures for bone implants: fabrication, mechanical and in vitro biological properties. Acta biomaterialia 2010;6:3349-59.
[32] Dabrowski B, Swieszkowski W, Godlinski D, Kurzydlowski KJ. Highly porous titanium scaffolds for orthopaedic applications. Journal of biomedical materials research Part B, Applied biomaterials 2010;95:53-61.
[33] Delahanty LM, Grant RW, Wittenberg E, Bosch JL, Wexler DJ, Cagliero E, et al. Association of diabetes-related emotional distress with diabetes treatment in primary care patients with Type 2 diabetes. Diabetic medicine : a journal of the British Diabetic Association 2007;24:48-54.
[34] Holzwarth JM, Ma PX. Biomimetic nanofibrous scaffolds for bone tissue engineering. Biomaterials 2011;32:9622-9.
[35] Yeo A, Wong WJ, Khoo HH, Teoh SH. Surface modification of PCL-TCP scaffolds improve interfacial mechanical interlock and enhance early bone formation: an in vitro and in vivo characterization. Journal of biomedical materials research Part A 2010;92:311-21.
[36] Teoh SH. Engineering materials for biomedical applications. 2004.
[37] Giannoudis PV, Dinopoulos H, Tsiridis E. Bone substitutes: an update. Injury 2005;36 Suppl 3:S20-7.
[38] McAndrew MP, Gorman PW, Lange TA. Tricalcium phosphate as a bone graft substitute in trauma: preliminary report. Journal of orthopaedic trauma 1988;2:333-9.
[39] El Ghannam A. Bone reconstruction: from bioceramics to tissue engineering. Expert review of medical devices 2005;2:87-101.
[40] Jones JR, Ehrenfried LM, Hench LL. Optimising bioactive glass scaffolds for bone tissue engineering. Biomaterials 2006;27:964-73.
[41] Logeart-Avramoglou D, Anagnostou F, Bizios R, Petite H. Engineering bone: challenges and obstacles. Journal of cellular and molecular medicine 2005;9:72-84.

[42] Kneser U, Schaefer DJ, Polykandriotis E, Horch RE. Tissue engineering of bone: the reconstructive surgeon's point of view. Journal of cellular and molecular medicine 2006;10:7-19.
[43] Hutmacher DW. Scaffolds in tissue engineering bone and cartilage. Biomaterials 2000;21:2529-43.
[44] van Tienen TG, Heijkants RG, Buma P, de Groot JH, Pennings AJ, Veth RP. Tissue ingrowth and degradation of two biodegradable porous polymers with different porosities and pore sizes. Biomaterials 2002;23:1731-8.
[45] Yang S, Leong KF, Du Z, Chua CK. The design of scaffolds for use in tissue engineering. Part I. Traditional factors. Tissue engineering 2001;7:679-89.
[46] Zeltinger J, Sherwood JK, Graham DA, Mueller R, Griffith LG. Effect of pore size and void fraction on cellular adhesion, proliferation, and matrix deposition. Tissue engineering 2001;7:557-72.
[47] Robinson BP, Hollinger JO, Szachowicz EH, Brekke J. Calvarial bone repair with porous D,L-polylactide. Otolaryngology--head and neck surgery : official journal of American Academy of Otolaryngology-Head and Neck Surgery 1995;112:707-13.
[48] Brauker JH, Carr-Brendel VE, Martinson LA, Crudele J, Johnston WD, Johnson RC. Neovascularization of synthetic membranes directed by membrane microarchitecture. Journal of biomedical materials research 1995;29:1517-24.
[49] Whang K, Healy KE, Elenz DR, Nam EK, Tsai DC, Thomas CH, et al. Engineering bone regeneration with bioabsorbable scaffolds with novel microarchitecture. Tissue engineering 1999;5:35-51.
[50] Oh SH, Park IK, Kim JM, Lee JH. In vitro and in vivo characteristics of PCL scaffolds with pore size gradient fabricated by a centrifugation method. Biomaterials 2007;28:1664-71.
[51] Karageorgiou V, Kaplan D. Porosity of 3D biomaterial scaffolds and osteogenesis. Biomaterials 2005;26:5474-91.
[52] Muschler GF, Nakamoto C, Griffith LG. Engineering principles of clinical cell-based tissue engineering. The Journal of bone and joint surgery American volume 2004;86-A:1541-58.
[53] Singh H, Teoh SH, Low HT, Hutmacher DW. Flow modelling within a scaffold under the influence of uni-axial and bi-axial bioreactor rotation. Journal of biotechnology 2005;119:181-96.
[54] Zein I, Hutmacher DW, Tan KC, Teoh SH. Fused deposition modeling of novel scaffold architectures for tissue engineering applications. Biomaterials 2002;23:1169-85.
[55] Williams JM, Adewunmi A, Schek RM, Flanagan CL, Krebsbach PH, Feinberg SE, et al. Bone tissue engineering using polycaprolactone scaffolds fabricated via selective laser sintering. Biomaterials 2005;26:4817-27.
[56] Hollister SJ. Porous scaffold design for tissue engineering. Nature materials 2005;4:518-24.
[57] Petite H, Viateau V, Bensaid W, Meunier A, de Pollak C, Bourguignon M, et al. Tissue-engineered bone regeneration. Nature biotechnology 2000;18:959-63.
[58] Jain RK, Au P, Tam J, Duda DG, Fukumura D. Engineering vascularized tissue. Nature biotechnology 2005;23:821-3.
[59] Malda J, Rouwkema J, Martens DE, Le Comte EP, Kooy FK, Tramper J, et al. Oxygen gradients in tissue-engineered PEGT/PBT cartilaginous constructs: measurement and modeling. Biotechnology and bioengineering 2004;86:9-18.
[60] Liu Y, Teoh SH, Chong MS, Lee ES, Mattar CN, Randhawa NK, et al. Vasculogenic and osteogenesis-enhancing potential of human umbilical cord blood endothelial colony-forming cells. Stem cells 2012;30:1911-24.
[61] Weiss S, Zimmermann G, Pufe T, Varoga D, Henle P. The systemic angiogenic response during bone healing. Archives of orthopaedic and trauma surgery 2009;129:989-97.

[62] Kaigler D, Wang Z, Horger K, Mooney DJ, Krebsbach PH. VEGF scaffolds enhance angiogenesis and bone regeneration in irradiated osseous defects. Journal of bone and mineral research : the official journal of the American Society for Bone and Mineral Research 2006;21:735-44.
[63] Hutmacher DW, Garcia AJ. Scaffold-based bone engineering by using genetically modified cells. Gene 2005;347:1-10.
[64] Fielding GA, Bandyopadhyay A, Bose S. Effects of silica and zinc oxide doping on mechanical and biological properties of 3D printed tricalcium phosphate tissue engineering scaffolds. Dental materials : official publication of the Academy of Dental Materials 2012;28:113-22.
[65] Tarafder S, Balla VK, Davies NM, Bandyopadhyay A, Bose S. Microwave-sintered 3D printed tricalcium phosphate scaffolds for bone tissue engineering. Journal of tissue engineering and regenerative medicine 2012.
[66] Xue W, Krishna BV, Bandyopadhyay A, Bose S. Processing and biocompatibility evaluation of laser processed porous titanium. Acta biomaterialia 2007;3:1007-18.
[67] Seyednejad H, Gawlitta D, Dhert WJ, van Nostrum CF, Vermonden T, Hennink WE. Preparation and characterization of a three-dimensional printed scaffold based on a functionalized polyester for bone tissue engineering applications. Acta Biomater 2011;7:1999-2006.
[68] Banfi A, Bianchi G, Notaro R, Luzzatto L, Cancedda R, Quarto R. Replicative aging and gene expression in long-term cultures of human bone marrow stromal cells. Tissue engineering 2002;8:901-10.
[69] Banfi A, Muraglia A, Dozin B, Mastrogiacomo M, Cancedda R, Quarto R. Proliferation kinetics and differentiation potential of ex vivo expanded human bone marrow stromal cells: Implications for their use in cell therapy. Experimental hematology 2000;28:707-15.
[70] Dupont KM, Sharma K, Stevens HY, Boerckel JD, Garcia AJ, Guldberg RE. Human stem cell delivery for treatment of large segmental bone defects. Proceedings of the National Academy of Sciences of the United States of America 2010;107:3305-10.
[71] Arinzeh TL, Peter SJ, Archambault MP, van den Bos C, Gordon S, Kraus K, et al. Allogeneic mesenchymal stem cells regenerate bone in a critical-sized canine segmental defect. The Journal of bone and joint surgery American volume 2003;85-A:1927-35.
[72] Bensaid W, Oudina K, Viateau V, Potier E, Bousson V, Blanchat C, et al. De novo reconstruction of functional bone by tissue engineering in the metatarsal sheep model. Tissue engineering 2005;11:814-24.
[73] Briggs T, Treiser MD, Holmes PF, Kohn J, Moghe PV, Arinzeh TL. Osteogenic differentiation of human mesenchymal stem cells on poly(ethylene glycol)-variant biomaterials. Journal of biomedical materials research Part A 2009;91:975-84.
[74] Pittenger MF, Mackay AM, Beck SC, Jaiswal RK, Douglas R, Mosca JD, et al. Multilineage potential of adult human mesenchymal stem cells. Science 1999;284:143-7.
[75] Caplan AI. Adult mesenchymal stem cells for tissue engineering versus regenerative medicine. Journal of cellular physiology 2007;213:341-7.
[76] Gastens MH, Goltry K, Prohaska W, Tschope D, Stratmann B, Lammers D, et al. Good manufacturing practice-compliant expansion of marrow-derived stem and progenitor cells for cell therapy. Cell transplantation 2007;16:685-96.
[77] Portner R, Nagel-Heyer S, Goepfert C, Adamietz P, Meenen NM. Bioreactor design for tissue engineering. Journal of bioscience and bioengineering 2005;100:235-45.
[78] Martin I, Wendt D, Heberer M. The role of bioreactors in tissue engineering. Trends in biotechnology 2004;22:80-6.

[79] Alvarez-Barreto JF, Linehan SM, Shambaugh RL, Sikavitsas VI. Flow perfusion improves seeding of tissue engineering scaffolds with different architectures. Annals of biomedical engineering 2007;35:429-42.
[80] Wendt D, Marsano A, Jakob M, Heberer M, Martin I. Oscillating perfusion of cell suspensions through three-dimensional scaffolds enhances cell seeding efficiency and uniformity. Biotechnology and bioengineering 2003;84:205-14.
[81] Grayson WL, Bhumiratana S, Cannizzaro C, Chao PH, Lennon DP, Caplan AI, et al. Effects of initial seeding density and fluid perfusion rate on formation of tissue-engineered bone. Tissue engineering Part A 2008;14:1809-20.
[82] Yang J, Cao C, Wang W, Tong X, Shi D, Wu F, et al. Proliferation and osteogenesis of immortalized bone marrow-derived mesenchymal stem cells in porous polylactic glycolic acid scaffolds under perfusion culture. Journal of biomedical materials research Part A 2010;92:817-29.
[83] Wendt D, Stroebel S, Jakob M, John GT, Martin I. Uniform tissues engineered by seeding and culturing cells in 3D scaffolds under perfusion at defined oxygen tensions. Biorheology 2006;43:481-8.
[84] Yeatts AB, Fisher JP. Bone tissue engineering bioreactors: dynamic culture and the influence of shear stress. Bone 2011;48:171-81.
[85] Volkmer E, Drosse I, Otto S, Stangelmayer A, Stengele M, Kallukalam BC, et al. Hypoxia in static and dynamic 3D culture systems for tissue engineering of bone. Tissue engineering Part A 2008;14:1331-40.
[86] Meinel L, Karageorgiou V, Fajardo R, Snyder B, Shinde-Patil V, Zichner L, et al. Bone tissue engineering using human mesenchymal stem cells: effects of scaffold material and medium flow. Ann Biomed Eng 2004;32:112-22.
[87] Wang TW, Wu HC, Wang HY, Lin FH, Sun JS. Regulation of adult human mesenchymal stem cells into osteogenic and chondrogenic lineages by different bioreactor systems. Journal of biomedical materials research Part A 2009;88:935-46.
[88] Zhang ZY, Teoh SH, Chong WS, Foo TT, Chng YC, Choolani M, et al. A biaxial rotating bioreactor for the culture of fetal mesenchymal stem cells for bone tissue engineering. Biomaterials 2009;30:2694-704.
[89] Grayson WL, Frohlich M, Yeager K, Bhumiratana S, Chan ME, Cannizzaro C, et al. Engineering anatomically shaped human bone grafts. Proceedings of the National Academy of Sciences of the United States of America 2010;107:3299-304.
[90] Zhao F, Chella R, Ma T. Effects of shear stress on 3-D human mesenchymal stem cell construct development in a perfusion bioreactor system: Experiments and hydrodynamic modeling. Biotechnology and bioengineering 2007;96:584-95.
[91] Bilodeau K, Mantovani D. Bioreactors for tissue engineering: focus on mechanical constraints. A comparative review. Tissue engineering 2006;12:2367-83.
[92] Bancroft GN, Sikavitsas VI, Mikos AG. Design of a flow perfusion bioreactor system for bone tissue-engineering applications. Tissue engineering 2003;9:549-54.
[93] Sikavitsas VI, Temenoff JS, Mikos AG. Biomaterials and bone mechanotransduction. Biomaterials 2001;22:2581-93.
[94] Rubin J, Rubin C, Jacobs CR. Molecular pathways mediating mechanical signaling in bone. Gene 2006;367:1-16.
[95] Grellier M, Bareille R, Bourget C, Amedee J. Responsiveness of human bone marrow stromal cells to shear stress. Journal of tissue engineering and regenerative medicine 2009;3:302-9.
[96] Godara P. Design of bioreactor for mesenchymal stem cells tissue engineering. J Chem Technol Biotechnol 2008;83:408-20.

[97] Sikavitsas VI, Bancroft GN, Mikos AG. Formation of three-dimensional cell/polymer constructs for bone tissue engineering in a spinner flask and a rotating wall vessel bioreactor. Journal of biomedical materials research 2002;62:136-48.
[98] Ichinohe N, Takamoto T, Tabata Y. Proliferation, osteogenic differentiation, and distribution of rat bone marrow stromal cells in nonwoven fabrics by different culture methods. Tissue engineering Part A 2008;14:107-16.
[99] Terai H. In vitro engineering of bone using a rotational oxygen-permeable bioreactor system. Mater Sci Eng 2002;20:3-8.
[100] Shin M, Yoshimoto H, Vacanti JP. In vivo bone tissue engineering using mesenchymal stem cells on a novel electrospun nanofibrous scaffold. Tissue Eng 2004;10:33-41.
[101] Yoshimoto H, Shin YM, Terai H, Vacanti JP. A biodegradable nanofiber scaffold by electrospinning and its potential for bone tissue engineering. Biomaterials 2003;24:2077-82.
[102] Song K, Liu T, Cui Z, Li X, Ma X. Three-dimensional fabrication of engineered bone with human bio-derived bone scaffolds in a rotating wall vessel bioreactor. Journal of biomedical materials research Part A 2008;86:323-32.
[103] Zhang ZY, Teoh SH, Teo EY, Khoon Chong MS, Shin CW, Tien FT, et al. A comparison of bioreactors for culture of fetal mesenchymal stem cells for bone tissue engineering. Biomaterials 2010;31:8684-95.
[104] Wang L, Hu YY, Wang Z, Li X, Li DC, Lu BH, et al. Flow perfusion culture of human fetal bone cells in large beta-tricalcium phosphate scaffold with controlled architecture. J Biomed Mater Res A 2009;91:102-13.
[105] Sikavitsas VI, Bancroft GN, Lemoine JJ, Liebschner MA, Dauner M, Mikos AG. Flow perfusion enhances the calcified matrix deposition of marrow stromal cells in biodegradable nonwoven fiber mesh scaffolds. Annals of biomedical engineering 2005;33:63-70.
[106] Bancroft GN, Sikavitsas VI, van den Dolder J, Sheffield TL, Ambrose CG, Jansen JA, et al. Fluid flow increases mineralized matrix deposition in 3D perfusion culture of marrow stromal osteoblasts in a dose-dependent manner. Proceedings of the National Academy of Sciences of the United States of America 2002;99:12600-5.
[107] Melchels FP, Barradas AM, van Blitterswijk CA, de Boer J, Feijen J, Grijpma DW. Effects of the architecture of tissue engineering scaffolds on cell seeding and culturing. Acta biomaterialia 2010;6:4208-17.
[108] Hulbert SF, Young FA, Mathews RS, Klawitter JJ, Talbert CD, Stelling FH. Potential of ceramic materials as permanently implantable skeletal prostheses. Journal of biomedical materials research 1970;4:433-56.
[109] Zardiackas LD, Parsell DE, Dillon LD, Mitchell DW, Nunnery LA, Poggie R. Structure, metallurgy, and mechanical properties of a porous tantalum foam. Journal of biomedical materials research 2001;58:180-7.
[110] Chen JP, Chang YS. Preparation and characterization of composite nanofibers of polycaprolactone and nanohydroxyapatite for osteogenic differentiation of mesenchymal stem cells. Colloids and surfaces B, Biointerfaces 2011;86:169-75.
[111] Sarkar MR, Augat P, Shefelbine SJ, Schorlemmer S, Huber-Lang M, Claes L, et al. Bone formation in a long bone defect model using a platelet-rich plasma-loaded collagen scaffold. Biomaterials 2006;27:1817-23.
[112] Ciardelli G, Chiono V, Vozzi G, Pracella M, Ahluwalia A, Barbani N, et al. Blends of poly-(epsilon-caprolactone) and polysaccharides in tissue engineering applications. Biomacromolecules 2005;6:1961-76.
[113] Leong KF, Wiria FE, Chua CK, Li SH. Characterization of a poly-epsilon-caprolactone polymeric drug delivery device built by selective laser sintering. Bio-medical materials and engineering 2007;17:147-57.

[114] Rai B, Ho KH, Lei Y, Si-Hoe KM, Jeremy Teo CM, Yacob KB, et al. Polycaprolactone-20% tricalcium phosphate scaffolds in combination with platelet-rich plasma for the treatment of critical-sized defects of the mandible: a pilot study. Journal of oral and maxillofacial surgery : official journal of the American Association of Oral and Maxillofacial Surgeons 2007;65:2195-205.
[115] Yeo A, Sju E, Rai B, Teoh SH. Customizing the degradation and load-bearing profile of 3D polycaprolactone-tricalcium phosphate scaffolds under enzymatic and hydrolytic conditions. Journal of biomedical materials research Part B, Applied biomaterials 2008;87:562-9.

Acknowledgments

The author would like to acknowledge Dr. Giacomo Cattaruzzi and Dr. Massimo Moretti of VBC spa.

Arthroscopic Mosaicplasty for Osteochondral Lesions of the Knee: Computer-Assisted Navigation Versus Freehand Technique

Paolo Di Benedetto, M.D., Mustafa Citak, M.D., Daniel Kendoff, M.D., Padhraig F. O'Loughlin, M.D., Eduardo M. Suero, M.D., Andrew D. Pearle, M.D., and Dimitrios Koulalis, M.D.

Purpose: The purpose of this study was to compare a freehand arthroscopic approach versus mosaicplasty for treatment of osteochondral lesions of the knee with a navigated arthroscopic technique. **Methods:** Four whole cadaveric lower limbs were used. A conventional navigation system was used in combination with an autologous osteochondral graft transplantation system (Osteochondral Autograft Transfer System [OATS]; Arthrex, Naples, FL). The congruity of the articular surface was measured with the navigation probe to detect any difference between the surface created by the grafts and the surface of the femoral condyle surrounding them. The angle relates to a line perpendicular to the articular surface. This line is made by the cutting instrument for graft harvesting and insertion and the articular surface. **Results:** The mean angle of graft harvest was 3.4° (range, 0° to 10°) in the navigated group versus 14.8° (range, 6° to 26°) in the freehand group ($P < .0003$). The mean angle for recipient-site coring was 1.5° (range, 0° to 5°) in the navigated group versus 12.6° (range, 4° to 17°) in the freehand group ($P < .0003$). The mean angle of graft placement was 2° (range, 1° to 5°) in the navigated group versus 10.8° (range, 5° to 15°) in the freehand group ($P = .0002$). The mean protrusion height of the plug was 0.23 mm (range, 0.1 to 0.5 mm; SD, 0.16) in the navigated group versus 0.34 mm (range, 0.0 to 0.7 mm; SD, 0.25) in the freehand group ($P = .336$). **Conclusions:** Computer-assisted arthroscopic mosaicplasty for treatment of osteochondral lesions in the cadaveric model presented in this study allows permanent visualization of the angle of recipient-site preparation, the depth of the donor plug and the recipient plug, and the angle of insertion of the graft at the recipient site. **Clinical Relevance:** This study shows evidence of potentially greater precision and reproducibility of navigated arthroscopic mosaicplasty when compared with an arthroscopic freehand technique in a cadaveric model. However, true clinical outcome benefit will only be elucidated upon performance of appropriate clinical studies.

Osteochondral transplantation with either single or multiple grafts (i.e., mosaicplasty) has been used widely for the treatment of osteochondral defects.[1,2] In general, autografts have been used to treat smaller (<200 mm^2) full-thickness chondral defects, with allografts used for larger osteochondral lesions.[3] The Osteochondral Autograft Transfer System (OATS) (Arthrex, Naples, FL) procedure involves removing

From the Clinic of Orthopaedics and Traumatology, University of Udine (P.D.), Udine, Italy; Department of Orthopaedic Surgery, Hospital for Special Surgery (P.D., M.C., D.K., P.F.O., E.M.S., A.D.P.), New York, New York, U.S.A.; and First Orthopaedic Department, University of Athens, University Hospital "Attikon" (D.K.), Athens, Greece.

Paolo Di Benedetto and Mustafa Citak contributed equally to this work.

The authors report that they have no conflicts of interest in the authorship and publication of this article.

Received June 3, 2011; accepted February 16, 2012.

Address correspondence to Mustafa Citak, M.D., Department of Orthopaedic Surgery, Hospital for Special Surgery, 535 East 70th Street, New York, NY, 10021, U.S.A. E-mail: mcitak@gmx.de

0749-8063/11349/$36.00

doi:10.1016/j.arthro.2012.02.013

cylindrical osteochondral grafts from lesser weight-bearing areas of the articular cartilage with subsequent transfer to debrided full-thickness defects. This procedure may be performed through an open or arthroscopic approach.

Restoration of joint congruity by the mosaicplasty technique is a technically demanding procedure. However, with attention to detail, articular surface congruency can be achieved. Bobic[4] has shown that graft harvesting and insertion should be perpendicular to the articular surface and deviation from this angle may compromise the ultimate outcome. Grafts should also be implanted to be flush with the joint surface to avoid graft micromotion and facilitate rapid incorporation.[5] Reproducible insertion angles may be negatively influenced by the 30° arthroscope typically used in arthroscopic procedures. Potential complications include the migration of donor plugs with resultant loose body formation and damage to the weight-bearing area during graft harvest.

Computer-assisted navigation facilitates 3-dimensional accuracy and precise control for several orthopaedic procedures in the spine, hip, knee, and ankle.[6-13] The overall accuracy for orthopaedic applications with integration of this technology may be up to within 1 mm or 1°.[14] In a previous cadaveric study performed by us, navigated perpendicular placement of cylindrical osteochondral grafts was shown to be significantly more precise than with a freehand technique using an open surgical approach.[15] This accurate placement was shown to be reproducible, and the height of the plug after insertion was shown to be significantly more congruent with the surrounding joint surface than with the freehand technique.

The purpose of this study was to compare a freehand, minimally invasive arthroscopic approach versus mosaicplasty for treatment of osteochondral lesions of the knee with a navigated, minimally invasive arthroscopic technique. The fundamental difference compared with our previous study is the use of a minimally invasive arthroscopic approach instead of an open surgical technique.

Therefore the hypothesis of this study was 2-fold: (1) Computer-navigated arthroscopic insertion of osteochondral grafts in the knee joint would provide more accurate positioning as regards perpendicularity of the grafts in relation to the joint surface, compared with a freehand arthroscopic technique. (2) Congruity of the recipient articular surface would be greater after a navigated technique than a freehand technique, that is, the height of the graft, or its "proudness," would be minimal such that optimal joint surface congruity would be achieved with the graft flush to the surface.

FIGURE 1. Experimental setup with customized reference markers, harvest and donor guides, arthroscopy screens, and navigation display unit.

METHODS

Operative Technique

Four fresh-frozen whole cadaveric lower limbs without prior injuries, pathology, or a history of knee surgery were acquired for the study. Two were designated for the navigated technique and two for a freehand procedure. A conventional image-free navigation system (Praxim, Grenoble, France) was used in combination with a conventional system for autologous osteochondral graft transplantation in the knee joint (OATS Sterile, Single-Use Kit; Arthrex) (Fig 1). The software provided information concerning the angle of the cutting instrument on the articular surface. The cadaveric lower limbs were thawed overnight at room temperature before the procedure. Next, the femoral head was fixed in a customized lower limb–holding device. After rigid intraosseous fixation of femoral and tibial reference markers with 3.5-mm Schanz screws, the lower limb registration process was performed (Fig 2). Modified software designed for anterior cruciate reconstruction was used. A customized reference tracker was fixed to both the OATS recipient and donor hollow guides, thus referencing the exact position of these instruments in relation to the articular surface. The image-free navigation system registration process included the hip center and defined tibial and femoral cutaneous landmarks, and through arthroscopic visualization, a bone-morphing

FIGURE 2. Arthroscopic registration of joint surfaces with navigation probe: (A) medial femoral condyle, (B) intercondylar notch, and (C) lateral femoral condyle.

algorithm for defined femoral intra-articular landmarks was performed, including donor and recipient sites of the lateral and medial aspects of the femoral trochlea and the lateral and medial femoral condyles. Consequently, the position of the guide tip and its depth in relation to the articular surface could be visualized continuously.

Surgical Technique

Surgery was performed arthroscopically in both the navigated and non-navigated procedures by the same surgeon. The diameter of the graft-harvesting tool was 8 mm, and this device was placed to a depth of 15 mm. Three grafts that were taken from the lesser weight-bearing zone of the lateral femoral condyle were transferred to the weight-bearing zone of the medial femoral condyle. Two grafts that were taken from the lesser weight-bearing zone of the medial condyle were transferred to the weight-bearing zone of the lateral femoral condyle. Thus, in each knee, 5 harvests were performed, in addition to 5 transplants, so that 10 such procedures were performed in each group. Navigation ensured that the harvesting device was perpendicular to the articular surface. By use of a mallet, the harvester was driven into the bone to a depth of 15 mm. The harvester containing the cylindrical osteochondral graft was then removed by rotating the T-handle sharply by 90° twice to score and dislodge the graft.

The recipient site was prepared with the recipient tool. This has a similar T-handle construct, but critically, the instrument forms a recipient site that has a diameter that is 1 mm less than that of the donor harvester so that the transplanted graft will fit tightly into the recipient site, achieving a "press-fit" arrangement. The osteochondral graft was advanced into the pre-cored area under the guidance of navigation at an angle of 90° to the articular surface, which was calculated as an angle of 0° for the instrument's longitudinal axis. The congruity of the articular surface was measured with the navigation probe to detect any difference between the surface created by the grafts and the surface of the femoral condyle surrounding them. Registration of anatomic points is an integral step in navigation. Logging of the coordinates of the articular surface facilitates identification and quantification of articular incongruities. Graft height was calculated from the coordinates registered for the surrounding articular surface. Positive or negative values were used to reflect the congruity (protrusion or subsidence of the graft) to the surrounding cartilage surface.

The same procedure was then performed arthroscopically but without the aid of navigation and thus in a freehand fashion. Once graft transplantation was completed without navigation, the congruity of the articular surface was measured again in a similar fashion to the navigated procedure to allow a comparison.

Navigation thus served in 1 arm of the study as an aid to correct osteochondral graft placement and also served as a postprocedural assessment tool for both the navigated and non-navigated groups. It facilitated the following measurements:

- Angle of graft harvesting at the donor site, which was measured with respect to a perpendicular line at the joint surface
- Angle of the recipient-site coring (the angle between the bone core removed from the site that is to receive an osteochondral graft and this site's surface)
- Angle of graft placement (the angle between the osteochondral graft and the recipient site, as it is placed)

- Depth of graft harvest (which gives an indirect measurement of the height of the osteochondral graft harvested from a donor site) and graft placement (the depth to which the osteochondral graft is placed; ideally, this graft should be flush [i.e., the recipient coring depth should match the graft-harvesting depth]).

After completion of the procedures, surface congruity (i.e., whether the graft was "flush" with the surrounding area) was confirmed arthroscopically. Perpendicularity in both recipient-site coring and graft harvest is desirable to have the most congruent graft placement possible and hence optimal joint surface congruity.

Statistical Analysis

All variables were expressed in terms of mean ± standard deviation of the mean. An unpaired Student *t* test was performed when the data had a normally Gaussian distribution; otherwise, the Mann-Whitney test was used. The Shapiro-Wilk normality test was performed to ascertain whether the data were normally distributed. For all tests, $P < .05$ was considered statistically significant. Statistical analysis was carried out by means of a statistical software package (GraphPad Prism, version 4.1; GraphPad Software, La Jolla, CA).

RESULTS

Considering an optimal angle as 0° from normal to the articular surface in midlateral and anterior-posterior, the mean angle of graft harvest was 3.4° (range, 0° to 10°; SD, 3.10°) in the navigated group versus 14.8° (range, 6° to 26°; SD, 7.53°) in the freehand group ($P < .0003$) (Fig 3). The mean angle for recipient-site coring was 1.50° (range, 0° to 5°; SD, 1.65°) in the navigated group versus 12.60° (range, 4° to 17°; SD, 3.98°) in the freehand group ($P < .0003$) (Fig 4). The mean angle of graft placement was 2.0° (range, 1° to 5°; SD, 1.25°) in the navigated group versus 10.8° (range, 5° to 15°; SD, 3.23°) in the freehand group ($P = .0002$) (Fig 5).

The mean difference between the angle of graft harvest and the angle of graft placement was 2.40° (range, 0° to 8°; SD, 2.46°) in the navigated group versus 7° (range, 1° to 16°; SD, 5.19°) in the freehand group ($P = .0207$). Meanwhile, the mean difference between the angle of recipient-site coring and the angle of graft placement was 0.90° (range, 0° to 2°; SD, 0.74°) in the navigated group versus 9.2° (range,

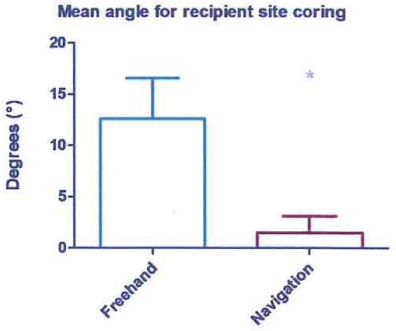

FIGURE 4. Varying angles of recipient-site coring between freehand technique and navigated technique. Asterisk, significant difference.

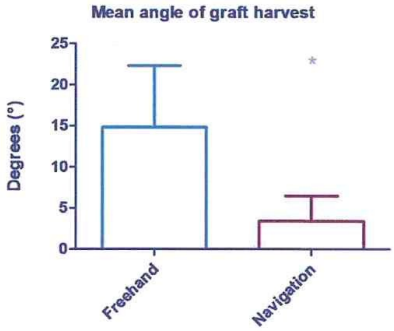

FIGURE 3. Varying angles of osteochondral plug harvest between freehand technique and navigated technique. Asterisk, significant difference.

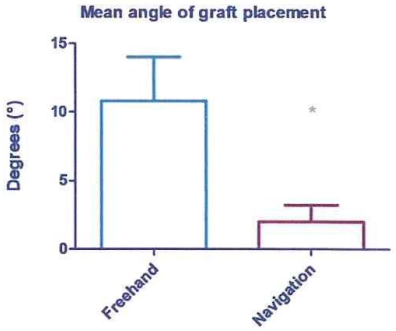

FIGURE 5. Varying angles of recipient-site plug transplant between freehand technique and navigated technique. Asterisk, significant difference.

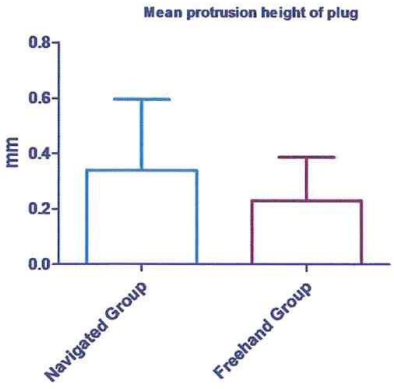

FIGURE 6. Mean protrusion height of plugs between freehand technique and navigated technique.

6° to 14°; SD, 2.57°) in the freehand group (P = .002).

The mean protrusion height of the plug was 0.23 mm (range, 0.1 to 0.5 mm; SD, 0.16 mm) in the navigated group versus 0.34 mm (range, 0.0 to 0.7 mm; SD, 0.25 mm) in the freehand group (P = .336) (Fig 6).

DISCUSSION

Achieving joint congruency in the treatment of osteochondral lesions by graft transplantation is challenging. For small lesions, many techniques allow the local radius of curvature at the defect site to be restored. However, with larger lesions, it can be difficult to achieve surface congruity, especially with arthroscopic approaches. In the OATS procedure, this can be difficult when just 1 cylindrical osteochondral autograft is used, but the challenge is even greater when a mosaicplasty approach is adopted with a number of cylindrical osteochondral grafts harvested and placed in the injured region.

In a previous study performed by us, it was evident that, with the aid of navigation, mosaicplasty for very large defects (i.e., >200 mm^2) was possible.[15] Critically, each transplanted plug must be harvested at a certain angle to match the local radius of articular surface curvature, and this is made possible by navigation technology. The plugs are implanted relatively parallel to each other while maintaining perpendicularity to the adjacent joint surface with press fitting into the prepared defect. This press fit is facilitated by the 1-mm difference in the diameter of the harvesting instrument (8 mm) versus the recipient-site harvesting instrument (7 mm).

Chow et al.[16] and Marcacci et al.[17] established that both graft harvest and placement should be performed perpendicular to the articular surface and that deviating from such an approach could compromise the end result and impair osseointegration and surface matching. If the plug is malaligned with respect to the recipient site, it will require more energy to tamp it into place, with a consequent increase in the potential impaction injury to the cartilage.[18] Jakob et al.[19] stressed the importance of surface congruity. Hangody et al.[20] have also supported the importance of surface matching between the graft and recipient site.

The level with regard to the surrounding articular surface of the various plugs is another important factor. If a plug is placed too high or there are differences among various plug heights, generating a so-called organ pipe configuration, this can lead to unequal distribution of joint load.[5] This may cause abrasion of the plug surface and damage to the opposing joint surface. In contrast, those plugs that are denied normal physiological loading conditions in a situation where there is uneven plug height may be vulnerable to degeneration because of a lack of loading stimulus.[17] In addition to the overall height of the graft relative to the articular surface, the cartilage layer thickness should be considered such that the graft and recipient area cartilage thicknesses match. Ideal graft length is deemed to be approximately 15 mm, such that at least 10 mm of cancellous bone will be fixed within the recipient socket.

Cyst formation has been ascribed to plug instability and synovial fluid penetrating the subchondral bone. Whiteside et al.[21] have reported that the initial stability after plug transfer decreases by more than 50% after 1 week. These factors emphasize the necessity to provide as much stability as possible to the plugs during osteochondral transplantation. Other factors also play a critical role in maintaining a stable position, such as inter-plug and plug-host congruency, surface curvature, and differences in contact pressures. This finding reinforces the importance of articular surface congruity in the initial biomechanical state after osteochondral implantation, and we recommend that meticulous attention be paid to the perpendicular preparation of the graft site and the harvesting of grafts. We believe that computer navigation can aid the surgeon in achieving a perpendicular approach as well as optimal surface congruency.

Repositioning of the grafts may also lead to a loss of stability. The result of an unstable graft might be

either initial failure if the graft becomes loose or, by discrete loss of congruity, increased mechanical wear. The fact that reinsertion of grafts after pullout leads to a reduction of ultimate failure loads stresses the importance of careful intraoperative planning during osteochondral autografting. The surgeon must bear in mind that once a graft is extracted from the recipient defect to improve the graft position, press-fit stability will decrease. Computer navigation can provide accurate data on the direction of the grafts as well as the depth of the graft and graft recipient socket.

With standard techniques, even in open procedures, reproducibility of graft positioning can be difficult even for experienced surgeons. When one then considers performing mosaicplasty arthroscopically, the challenge is made even greater. However, in our study computer-assisted surgery showed greater precision during harvesting, recipient-site preparation, and plug placement. The navigated procedures also showed superior reproducibility. Thus we view navigation technology as an enabler when it comes to converting to an arthroscopic mosaicplasty procedure.

However, there are limitations to navigation technology. These include the necessity to apply invasive intraosseous reference markers; an increase in operative time because of the setup, including the registration process; and preliminary fixation of a reference marker to the OATS T-handle guide system. Use of computer-assisted technology is more expensive than conventional techniques. It would be difficult to justify installation of computer navigation hardware and software for OATS surgery alone. However, if such a system is also used for other applications such as anterior cruciate ligament reconstruction or high tibial osteotomy, this would be more reasonable. Of course, if there is a real clinical benefit with a more favorable outcome and durability of the grafts and graft sites, then such technology may be warranted despite financial and temporal costs. A further limitation of our study is that a small number of specimens were tested. Another limitation is that comparisons of accuracy between the navigated and freehand approaches, as well as the angle and depth of the graft, were assessed with the navigation system with the assumption that the presented values were accurate. A different analytic method such as 3-dimensional image analysis may be required to critically evaluate the accuracy of the navigated procedure.

This study highlights certain potential benefits in terms of precision and accuracy. However, true clinical outcome benefit will only be elucidated upon performance of appropriate clinical studies. On the contrary to our previous study, this study shows that even very large defects can be treated successfully with mosaicplasty assisted with navigation. The main problem with large lesions is to find appropriately large grafts. At this time, using autologous grafts in combination with synthetic grafts can overcome this problem.

CONCLUSIONS

Computer-assisted arthroscopic mosaicplasty for treatment of osteochondral lesions in the cadaveric model presented in this study allows permanent visualization of the angle of recipient-site preparation, the depth of the donor plug and the recipient plug, and the angle of insertion of the graft at the recipient site. This study shows evidence of potentially greater precision and reproducibility of navigated arthroscopic mosaicplasty when compared with an arthroscopic freehand technique in a cadaveric model.

REFERENCES

1. Hangody L, Füles P. Autologous osteochondral mosaicplasty for the treatment of full-thickness defects of weight-bearing joints: Ten years of experimental and clinical experience. *J Bone Joint Surg Am* 2003;85:25-32 (Suppl 2).
2. Hangody L, Kish G, Módis L, et al. Mosaicplasty for the treatment of osteochondritis dissecans of the talus: Two to seven year results in 36 patients. *Foot Ankle Int* 2001;22:552-558.
3. Emmerson BC, Görtz S, Jamali AA, Chung C, Amiel D, Bugbee WD. Fresh osteochondral allografting in the treatment of osteochondritis dissecans of the femoral condyle. *Am J Sports Med* 2007;35:907-914.
4. Bobic V. Arthroscopic osteochondral autograft transplantation in anterior cruciate ligament reconstruction: A preliminary clinical study. *Knee Surg Sports Traumatol Arthrosc* 1996;3:262-264.
5. Pearce SG, Hurtig MB, Clarnette R, Kalra M, Cowan B, Miniaci A. An investigation of 2 techniques for optimizing joint surface congruency using multiple cylindrical osteochondral autografts. *Arthroscopy* 2001;17:50-55.
6. Bailey C, Gul R, Falworth M, Zadow S, Oakeshott R. Component alignment in hip resurfacing using computer navigation. *Clin Orthop Relat Res* 2009;467:917-922.
7. Blattert TR, Springwald J, Glasmacher S, Siekmann H, Josten C. Computer-aided discectomy and corpectomy in anterior reconstruction of the injured thoracolumbar spine. A prospective, controlled clinical trial. *Unfallchirurg* 2008;111:878-885 (in German).
8. Kendoff D, Geerling J, Mahlke L, et al. Navigated Iso-C(3D)-based drilling of a osteochondral lesion of the talus. *Unfallchirurg* 2003;106:963-967 (in German).
9. Lützner J, Krummenauer F, Wolf C, Günther KP, Kirschner S. Computer-assisted and conventional total knee replacement: A comparative, prospective, randomised study with radiological and CT evaluation. *J Bone Joint Surg Br* 2008;90:1039-1044.
10. Mizu-Uchi H, Matsuda S, Miura H, Higaki H, Okazaki K, Iwamoto Y. Three-dimensional analysis of computed tomography-based navigation system for total knee arthroplasty: The

accuracy of computed tomography-based navigation system. *J Arthroplasty* 2009;24:1103-1110.
11. Pitto RP, Malak S, Anderson IA. Accuracy of a computer-assisted navigation system in resurfacing hip arthroplasty. *Int Orthop* 2009;33:391-395.
12. Romanowski JR, Swank ML. Imageless navigation in hip resurfacing: Avoiding component malposition during the surgeon learning curve. *J Bone Joint Surg Am* 2008;90:65-70 (Suppl 3).
13. Tjardes T, Paffrath T, Baethis H, et al. Computer assisted percutaneous placement of augmented iliosacral screws: A reasonable alternative to sacroplasty. *Spine* 2008;33:1497-1500.
14. Khadem R, Yeh CC, Sadeghi-Tehrani M, et al. Comparative tracking error analysis of five different optical tracking systems. *Comput Aided Surg* 2000;5:98-107.
15. Koulalis D, Di Benedetto P, Citak M, O'Loughlin P, Pearle AD, Kendoff DO. Comparative study of navigated versus freehand osteochondral graft transplantation of the knee. *Am J Sports Med* 2009;37:803-807.
16. Chow JC, Hantes ME, Houle JB, et al. Arthroscopic autogenous osteochondral transplantation for treating knee cartilage defects: A 2- to 5-year follow-up study. *Arthroscopy* 2004; 20:681-690.
17. Marcacci M, Uon E, Zaffagnini S, et al. Multiple osteochondral arthroscopic grafting (mosaicplasty) for cartilage defects of the knee: Prospective study results at 2-year follow-up. *Arthroscopy* 2005;21:462-470.
18. Wu JZ, Herzog W, Hasler EM. Inadequate placement of osteochondral plugs may induce abnormal stress-strain distributions in articular cartilage—Finite element simulations. *Med Eng Phys* 2002;24:85-97.
19. Jakob RP, Franz T, Gautier E, Mainil-Varlet P. Autologous osteochondral grafting in the knee: Indication, results, and reflections. *Clin Orthop Relat Res* 2002:170-184.
20. Hangody L, Ráthonyi GK, Duska Z, Vásárhelyi G, Füles P, Módis L. Autologous osteochondral mosaicplasty. Surgical technique. *J Bone Joint Surg Am* 2004;86:65-72 (Suppl 1).
21. Whiteside RA, Bryant JT, Jakob RP, Mainil-Varlet P, Wyss UP. Short-term load bearing capacity of osteochondral autografts implanted by the mosaicplasty technique: An in vitro porcine model. *J Biomech* 2003;36:1203-1208.